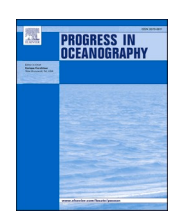
ELSEVIER

Contents lists available at ScienceDirect

Progress in Oceanography

journal homepage: www.elsevier.com/locate/pocean





Temporal dynamics of total microbial biomass and particulate detritus at Station ALOHA

David M. Karl ^{a,*}, Karin M. Björkman ^a, Matthew J. Church ^b, Lance A. Fujieki ^a, Eric M. Grabowski ^a, Ricardo M. Letelier ^c

- a Daniel K. Inouye Center for Microbial Oceanography: Research and Education, University of Hawai'i at Mānoa, Honolulu, HI 96822, USA
- ^b Flathead Lake Biological Station, University of Montana, Polson, MT 59860, USA
- ^c College of Earth, Ocean and Atmospheric Sciences, Oregon State University, Corvallis, OR 97331, USA

ARTICLE INFO

Keywords:
Microbial biomass
Carbon
ATP
Station ALOHA
Detritus
North Pacific Subtropical Gyre

ABSTRACT

Particulate adenosine-5'-triphosphate (P-ATP) and particulate carbon (PC) concentrations were measured on approximately monthly intervals throughout the upper water column (0-1000 m) over a 30-yr (1989-2018) period at Station ALOHA to track the seasonal-to-decadal variability in total microbial biomass and the dynamics of living-to-nonliving particulate organic matter pools. On selected cruises, samples were also collected to a depth of \sim 4800 m. P-ATP concentrations were relatively uniform (27–34 ng l^{-1}) throughout the upper euphotic zone (0–100 m) with a distinct peak at 45 m. P-ATP concentrations were significantly higher (p < 0.001) in summer (Jun-Aug) than in winter (Dec-Feb), especially between 45 and 100 m where the seasonal differences averaged 28%. Below 100 m, P-ATP concentrations decreased rapidly with depth to a 30-yr mean value of 3.5 ng ATP l^{-1} at 250 m, and then decreased more gradually to a 30-yr mean value of 0.9 ng ATP l^{-1} at 1000 m. Between 125 and 175 m, the seasonal peak in P-ATP shifted to spring (Mar-May), with minima in fall (Sep-Nov) and winter (Dec-Feb). No consistent seasonal variations in P-ATP were detected at depths > 175 m, suggesting a temporally stable habitat. Assuming a PC:P-ATP ratio of 250:1 (g g^{-1}), the 0–100 m, 100–250 m, and 250–1000 m, and 250–1 m depth-integrated microbial biomass estimates were 775, 425, and 350 mg C m⁻², respectively. Bathypelagic zone (>1000 m) P-ATP concentrations, based on a more limited data set than the upper portions of the water column, were low (0.4-0.7 ng ATP l-1). However, when integrated over the entire deep water habitat (1000–4800 m), bathypelagic zone microbial biomass was substantial (425 mg C m⁻²). Expressed as a percentage of total PC, microbial biomass ranged from \sim 30% in the upper euphotic zone to \sim 3% at depths >3000 m, emphasizing the preponderance of detrital PC throughout the entire water column. The total water column inventory of microbial biomass at Station ALOHA was 2 g C m $^{-2}$ compared to \sim 18 g C m $^{-2}$ for total suspended PC; approximately 50% of the total microbial biomass is resident in the aphotic zone (>175 m). Although daily gross primary production at Station ALOHA is on par with the total euphotic zone (0-175 m)-integrated microbial biomass (~1 g C m⁻² d⁻¹ and ~1 g C m⁻², respectively), the sources of C and energy fueling the substantial aphotic zone microbial biomass (\sim 1 g m $^{-2}$) are not well understood at the present time.

1. Introduction

More than half a century ago, Holm-Hansen and Booth (1966) presented a novel approach to estimate total microbial biomass in the sea via the quantitative determination of particulate adenosine-5'-triphosphate (P-ATP). The conceptual and analytical breakthroughs for the use of cellular ATP as a biomass indicator were enabled by two independent discoveries. In 1941, Fritz Lipmann reported that ATP was the primary

metabolic energy currency in living systems, and coined the term "high energy phosphate bond" to refer to the β - and γ -P anhydride bonds of ATP (Lipmann, 1941). Subsequent research on a broad variety of microorganisms (bacteria and protists) confirmed the central and universal role of ATP in cellular metabolism. A few years later, William McElroy reported that ATP was the substrate for the *Photinus pyralis* bioluminescence reaction, leading to the development of a sensitive and specific quantitative assay for ATP using the firefly luciferin-luciferase system

E-mail address: dkarl@hawaii.edu (D.M. Karl).

https://doi.org/10.1016/j.pocean.2022.102803

^{*} Corresponding author.

(McElrov, 1947).

Prior to the introduction of the ATP-biomass assay in 1966, measurement of ATP had been proposed as a method for the rapid detection of viable bacteria (Levin et al., 1964), and as a possible life detection experiment for exploration of Mars (Levin and Heim, 1965). This latter experiment, with the codename Diogenes, would complement Gulliver, the life detection experiment based on the production of ¹⁴C-labeled carbon dioxide from a variety of ¹⁴C-labeled organic substrates (Levin et al., 1962), which ultimately did travel to Mars aboard the 1976 Viking lander. It is unfortunate that Diogenes was not selected for this important astrobiological mission because the equivocal results from Gulliver are still being debated four decades later (Levin and Straat, 2016).

The ATP-biomass method had two critical assumptions: (1) a near constant biomass carbon (C)-to-ATP relationship (hereafter, C:ATP ratio) in all living organisms and (2) a rapid turnover of ATP following cell death and autolysis such that the presence of P-ATP in any given sample would be restricted to living organisms. While subsequent research has shown systematic changes in the C:ATP ratio under conditions of nutrient depletion, energy starvation, or other forms of metabolic stress (e.g., Dawes and Large, 1970; Amy et al., 1983), a common C:ATP ratio has been demonstrated for a broad range of marine microorganisms, and micrometazoans (<200 µm; Holm-Hansen, 1970a; 1973). When used in conjunction with simultaneous measurements of particulate C, nitrogen, and phosphorus (PC, PN, and PP, respectively), chlorophyll a (Chl a), deoxyribonucleic acid (DNA), and lipopolysaccharide (LPS), total microbial biomass can be apportioned into specific autotrophic and heterotrophic compartments, along with estimation of nonliving particulate organic detritus (Holm-Hansen et al., 1989; Christian and Karl, 1994; Karl and Dobbs, 1998; Henderikx-Freitas et al., 2021). Regarding the assumption of rapid ATP turnover, a short half-life outside of living cells is essential for distinguishing living from nonliving PC. Although cell-free ATP (so called dissolved ATP, D-ATP) has been reported in a variety of aquatic ecosystems (Koenings and Hooper, 1973; Azam and Hodson, 1977; Hodson et al., 1981; Nawrocki and Karl, 1989; Björkman and Karl, 2005), it is not likely to interfere with the measurement of P-ATP unless it adsorbs to nonliving particulate matter (inorganic or organic), or onto the filter, thereby rendering it part of the P-ATP pool. Holm-Hansen and Booth (1966) recognized this possibility even before D-ATP was shown to be a ubiquitous component of the marine dissolved organic matter pool, and showed that ATP extracted from bacteria and algae does not readily adsorb onto nonliving particulate debris. Still, the possibility remains that certain inorganic particles (e.g., resuspended sediment, clays, calcium carbonate, opal) could adsorb D-ATP leading to an overestimate of the P-ATP concentration in selected ecosystems if the adsorbed ATP resulted in light emission during the firefly bioluminescence reaction. This can, and should be evaluated for each environmental application, along with other potential interferences in the determination of P-ATP (Karl, 2007).

Over the past several decades, the P-ATP assay has been successfully applied to a large number of ecological studies to estimate total microbial biomass from near-freezing waters beneath the Ross Ice Shelf, Antarctica (Azam et al., 1979) to near-boiling waters of deep-sea hydrothermal vents (Karl et al., 1984), and everywhere in between. In general, P-ATP distributions in the open sea correlate with primary and secondary production, decreasing with distance from shore and depth in the water column (Karl and Dobbs, 1998). Marine habitats with strong seasonal phasing in primary production (e.g., high latitude regions) also have large (>10-fold) seasonal variations in euphotic zone P-ATP concentrations (Karl et al., 1991). Beyond the continental shelf and below the euphotic zone, P-ATP concentrations are uniformly low (<10 ng 1^{-1}), equivalent to a microbial biomass of $\sim 2-3 \,\mu g \, C \, l^{-1}$, with gradually decreasing values (to <1 ng ATP l^{-1}) at depths >2000 m (Holm-Hansen, 1970b; Karl et al., 1976; Karl and Dobbs, 1998), confirming the existence of microbial life throughout the water column.

Although PC sets an upper limit on total biomass-C, the proportion of living to total particulate C as derived from P-ATP decreases from 30 to

70% in surface waters to <10% below the euphotic zone (Holm-Hansen and Booth, 1966; Holm-Hansen, 1969, 1970b). Knowledge of the sources, distributions, and dynamics of living versus nonliving organic matter is vital to our understanding of the oceanic C cycle and to the functioning of the biological C pump. The present study was motivated by a quest for this knowledge, and was facilitated by the establishment of the open ocean time-series Station ALOHA in the North Pacific Subtropical Gyre (NPSG; Karl and Lukas, 1996). Herein we report data on the depth distributions and temporal dynamics of P-ATP, PC, PN, and complementary physical and biogeochemical properties that were collected on approximately monthly intervals over a 30-yr period (1989-2018) at Station ALOHA. We use P-ATP concentrations to constrain total microbial biomass distribution throughout the water column, and document seasonal and interannual changes that result from changes in the environmental controls on carbon and energy flow. It was confirmed that living microbial biomass was only a small percentage of total PC, ranging from \sim 30% in surface waters to \sim 3% in the abyss. Finally, we present the enigmatic finding that total depthintegrated microbial biomass (P-ATP) beneath the euphotic zone (>150 m) exceeds that within the euphotic zone by \sim 25%, and discuss the implications of C and energy flow required to support this inverted biomass pyramid.

2. Materials and methods

2.1. Field sampling strategies

All field sampling was conducted at Station ALOHA (22°45'N, 158°W), an oligotrophic, open ocean site in the eastern portion of the NPSG (Karl and Lukas, 1996). The main data set presented in this paper covers the period Jan 1989 to Dec 2018, corresponding to samples collected during Hawaii Ocean Time-series (HOT) cruises 3-308. We also report bathypelagic zone (>2000 m depth) P-ATP data collected on cruises 320-322 (Jul-Sep 2020; see below). Due to inclement weather or equipment failures, P-ATP samples were not collected on 12 cruises (7, 20, 21, 42, 43, 48, 207, 218, 228, 276, 299, and 308). Furthermore, P-ATP samples that were collected on 17 additional cruises (47, 50, 54, 59, 60, 64, 69, 79, 83, 86, 90, 115, 122-124, 139, and 174) failed to meet the quality control criterion established for this analysis (i.e., ATP check standards were outside of the ± 2 standard deviation envelope of the ATP control chart; see ATP assay section). This reduced the number of cruises in the Station ALOHA P-ATP database to 277 during the 30-yr observation period. Multiple profiles collected during a given cruise were treated as independent samples. In order to obtain direct comparisons of P-ATP with PC (and PN), we prepared a particulate matter database using the same 277 HOT cruises.

Because depth profile samples for each variable were collected on different hydrocasts (but at the same location) that were separated in time by up to 24 h, the two data sets are not synoptic, so submesoscale (1-10 km) spatial variations may preclude cast-to-cast comparisons. Furthermore, due to tidal and inertial oscillations (~31 h period at the latitude of Station ALOHA), the position of isopycnal surfaces in the lower portion of the euphotic zone can move vertically by 50 m, or more, during a single cruise (Karl et al., 2002). Hence, since our samples were collected at specific depths, rather than specific densities, the accuracy of direct comparison of variables is degraded relative to samples that might have been collected from the same cast or the same sample bottle. This is especially critical in the upper 150 m region of the water column where variations in the parameter concentrations and density gradients are the greatest. This source of error is minimized by averaging P-ATP and PC over a given depth range and in the derivation of climatologies, as we do herein.

For each P-ATP and PC (and PN) profile (note: PC and PN are measured from the same filter; see **Particulate C and N assay** section), water samples were collected at depths of 5, 25, 45, 75, 100, 125, 150, 200, and 250 m for all 277 cruises. For an initial 12-year period

(1988–2000, 98 cruises) we also sampled at 175, 500, 750, and 1000 m, but then terminated these four mesopelagic zone depths and replaced them with a 350 m sample (duplicate bottles for PC and PN, see below) from Nov 2000 through Dec 2018 (171 cruises). Additional bathypelagic zone (>2000 m) P-ATP samples were also collected on cruises 96, 154, and 320–322 (Aug 1998, Dec 2003, and Jul-Sep 2020, respectively.

Continuous measurements of conductivity, temperature, and depth (CTD), and dissolved oxygen were averaged over 2-m intervals in post-cruise data processing. Discrete water samples were also collected for inorganic and organic nutrients, rates of primary production using the ¹⁴C-bicarbonate method, and a variety of other core parameters and cruise metadata, all of which are publicly available (hahana.soest.hawa ii.edu/hot/hot-dogs/interface.html).

2.2. ATP assay

ATP was measured using the firefly bioluminescence reaction based on the peak height method of Karl and Holm-Hansen (1978). Typically, water samples for ATP analysis were collected in 12 l polyvinylchloride (PVC) bottles on a dedicated hydrocast, and processed as soon as the rosette arrived on deck. The volume of seawater processed for each P-ATP sample ranged from 1 l for the upper water column (<150 m) to 2 L at greater depths. The samples were drawn through a PVC tube fitted with an in-line 202-um Nitex® screen to remove any mesozooplankton and other large particles. The pre-screened water was collected in a clean 4 l polyethylene bottle that was first rinsed three times with ~100-200 ml of the sample. Triplicate subsamples from each depth were processed by filtration through a 47-mm diameter Whatman glass fiber filter (GF/F) to assess analytical variability. Since only a single PVC sample bottle was routinely collected from each depth, we cannot report field variability. The collected particulate materials were immediately extracted in 5 ml of boiling Tris[hydroxymethyl]aminomethane (TRIS) buffer (0.02 M, pH 7.4 at 25 $^{\circ}$ C) for 5 min to kill the cells, extract intracellular ATP, and inactivate ATP hydrolytic enzymes. The extracted samples were stored frozen (-20 °C) until analyzed at our shore-based laboratory. Lyophilized firefly lantern extract (FLE-250; Sigma-Aldrich Chemical Co.) was reconstituted with 25 ml of distilled water and allowed to stand at room temperature for at least 6 h, but no longer than 24 h, to reduce the background light emission. Approximately 1 h prior to use, this concentrated extract was diluted with 75 ml of sodium arsenate buffer (0.1 M, pH 7.4) and 75 ml of magnesium sulfate (0.04 M), and filtered through a GF/F filter to remove particulate materials. The peak height of light emission following the injection of either 0.8 ml of enzyme mixture into 0.2 ml sample (cruises 3-157) or 0.3 ml of enzyme mixture into 0.1 ml sample (cruises 158-307; see below) was recorded, along with the light emission from a series of ATP standards. The primary ATP standard was prepared from high-purity sodium salt of ATP (>99% pure; #A2383, Sigma-Aldrich Chemical Co.) at a concentration of 10 mg ATP in 10 ml sterile distilled water. The exact concentration of the ATP standard solution was determined by light absorption at 259 nm using a molar extinction coefficient (ϵ) of 15.4 \times 10³ mol⁻¹ cm⁻¹. Newly prepared stock solutions were compared with previously used stocks and, if the new stock differed by > |1%|, the dilution step was repeated until the agreement was within the acceptable range. Stock standards of 1 µg ATP ml⁻¹ were placed into polyethylene tubes and stored at $-20~^{\circ}\text{C}$ as 1 ml aliquots until needed. Working standards ranging from 0.1 to 100 ng ATP ml⁻¹ were prepared daily by diluting the stock standard in TRIS buffer (0.02 M, pH 7.4) immediately prior to use, and were discarded at the end of the day. During the course of this 30-yr study, we used several commercially available ATP photometers: SAI ATP photometer model 2000 (Jan 1989 - Apr 1990), Biospherical Instruments model 2000 (May 1990 - Mar 2004), and Turner Biosystems model 2020ⁿ (Apr 2004 – Nov 2018). The coefficient of variation for the triplicate analyses (CV = mean \div standard deviation \times 100%) ranged from <10% to >50%, with larger errors typically at greater depths where extracted ATP concentrations were at the lower end of the standard curve (<2 ng ml $^{-1}$). We also reviewed all triplicate determinations to detect outliers, using the method of Grubbs (1969) and an $\alpha=0.05$ criterion for rejection. Of the 8190 independent P-ATP determinations in our study, 390 (<5%) were flagged as outliers and were excluded from subsequent analyses.

2.3. Particulate C and N assay

Samples for PC/PN analyses were collected on a dedicated hydrocast using the same CTD-PVC bottle rosette system, and from the same target depths as for P-ATP. For samples collected at 25 and 125 m, the PC and PN determinations were replicated from the same PVC sample bottle; all other depths except for 350 m (see below) were single determinations. For the period Dec 2004 - Dec 2018, the % difference of the replicated sample determinations was: 25 m PC mean = 10.6%, SD = 14.6%, n = 138; PN mean = 8.2%, SD = 10.1%, n = 138; PC:PN molar ratio mean = 7.3%, SD = 9.5%, n = 138; 125 m PC mean = 11.7%, SD = 12.6%, n = 136; PN = 10.4%, SD = 10.2%, n = 136; and PC:PN molar ratio mean = 8.7%, SD = 8.2%, n = 136. For PC and PN determinations at 350 m, we processed duplicate PVC bottles from the same hydrocast to evaluate field replication. Since the 350 m sampling began in Dec 2004, the % difference between the replicated PVC sample bottle determinations was: PC mean = 26.1%, SD = 27.2%, n = 137; PN mean = 21.9%, SD = 22.3%, n = 137; and PC:PN molar ratio mean = 14.3%, SD = 13.5%, n = 13.5%

Water samples for subsequent analysis of particulate matter were pre-screened (202-µm Nitex® mesh) as for P-ATP, then filtered onto precombusted (450 °C, 4.5 h) 25-mm diameter GF/F filters, placed onto combusted tin foil contained in polystyrene Petri® dishes, and stored frozen (-20 °C) for shore-based analyses. After drying at 60 °C for 16 h, each filter and matched foil were rolled together and pressed into a pellet for elemental analysis. For the initial period (Jan – May 1989), samples were analyzed using a Hewlett-Packard model 185B CHN analyzer (Sharp, 1974) but, after cross-comparisons, a Perkin-Elmer model 2400 CN analyzer was employed for cruises 7-53 (Jun 1989 -Mar 1994), and a Europa Scientific SL analyzer for cruises 54-165 (Jun 1994 - Nov 2004; Hebel and Karl, 2001). Since Dec 2004, an Exeter Analytical Elemental Analyzer using a combustion temperature of 1020 °C has been employed. The primary standard for all HOT program samples, acetanilide (C₈H₉NO; molecular weight = 135.16; C:N molar ratio = 8.0), was also analyzed as a check standard in each sample run. For samples analyzed between 2005 and 2018, the mean C:N ratio of the check standard was 8.03 (SD = 0.25, n = 222). We also routinely analyzed an in-house secondary standard prepared from dried, pulverized >202 µm mesozooplankton collected at Station ALOHA. The main purpose of the secondary standard is to make sure that the sample combustion and reduction processes are as complete and reproducible with a complex field-collected sample as they are with the pure chemical standard. For samples analyzed between 2005 and 2018, the mean C:N molar ratio of the secondary standard was 4.82 (SD = 0.16, n = 237). All samples were corrected for combusted GF/F filter blanks. For the period 2005–2018, mean PC and PN blank values were 14.1 μg C (SD = 5.1, n = 444) and 1.2 μ g N (SD = 0.9, n = 444) per filter. As reported herein, our high-temperature combustion (1020 °C) PC analysis includes both organic and inorganic (i.e., calcium carbonate) C compounds. Suspended particulate inorganic C (PIC) is present in very low concentrations in the NPSG (Gordon, 1970, 1971; Karl et al., 2021) and can be considered negligible. This conclusion is supported by the low bulk PC: PN molar ratios (range 5.9–7.6) that have been reported throughout the year for the euphotic zone (0–150 m) at Station ALOHA (Hebel and Karl, 2001).

2.4. Statistical methodology

Depth integrations were calculated using the trapezoidal rule:

$$\int_{a}^{b} f(x)dz \approx \sum_{z=1}^{N} \frac{f(x_{z-1}) + f(x_{z})}{2} \Delta z$$
 (1)

where x corresponds to the parameter being integrated over the depth Z. When integrating from 5 m to the surface, the upper interval was considered to be homogeneously mixed. The total variance over the integration depth was calculated through error propagation as:

$$Var_{Total} = Z_{Surf}^{2} *Var(x_{Surf})/n_{Surf} + (Z_{2} - Z_{Surf})^{2} * (Var(x_{2})/n_{2} + Var(x_{Surf})/n_{Surf})/2^{2} + \dots + (Z_{final-1} - Z_{Sfinal})^{2} * (Var(x_{2final-1})/n_{final-1} + Var(x_{final})/n_{final})/2^{2}$$
(2)

where Z corresponds to depth, Var is the sample variance, and n corresponds to the sample size. The number of significant figures reported reflects the uncertainty of each value based on the sampling replication and the sensitivity of the measurement.

Seasonal climatologies were estimated using two approaches: one method calculated monthly means and variance from the 30-year record. Alternatively, mean seasonal cycles were derived from the complete 1989–2018 time series by fitting a fundamental frequency, equivalent to the annual cycle plus a first harmonic, to a generalized linear model of the full time-series (Keeling et al., 2004).

Reported annual values are derived as the mean and standard deviation of values collected during the corresponding calendar year. Seasons are defined as: winter (Dec-Feb), spring (Mar-May), summer (Jun-

Aug), and fall (Sep-Nov).

3. Results

3.1. Depth profiles and inventories of P-ATP, PC, and PN

The 30-yr mean P-ATP concentrations at Station ALOHA ranged from 27 to 34 ng l $^{-1}$ in the upper 0–100 m portion of the water column to 0.9–3.5 ng l $^{-1}$ in the mesopelagic zone (250–1000 m; Fig. 1a and Table 1). While mean P-ATP concentrations were nearly identical at 5 m and 100 m, there was a distinct, consistent subsurface peak in the mean P-ATP at 45 m (Fig. 1a and Table 1). The 0–100 m depth-integrated P-ATP inventory was 3.1 mg m $^{-2}$, which is equivalent to a microbial biomass of 775 mg C m $^{-2}$, assuming a C:ATP ratio of 250:1 (Table 2).

Below 100 m, P-ATP concentrations decreased through the lower portion of the euphotic zone and upper portion of the mesopelagic zone to a mean value of 3.5 ng ATP l^{-1} at 250 m, followed by a more gradual decrease to a mean value of 0.9 ng ATP l^{-1} at 1000 m (Fig. 1a and Table 1). The mean P-ATP concentration measured at 500 m (1.9 ng l^{-1}) was slightly higher than that measured at 350 m (1.6 ng l^{-1} ; Table 1). The mean P-ATP inventories for the 100–250 m and 250–1000 m regions were 1.7 and 1.4 mg m $^{-2}$, respectively, equivalent to microbial biomasses of 425 and 350 mg C m $^{-3}$, assuming a C:ATP ratio of 250:1 (Table 2). Water samples from the bathypelagic zone revealed very low P-ATP concentrations (\leq 0.7 ng l^{-1} ; Table 2), similar to previous reports from Station Gollum located at 22°10′N, 158°W (47 km due north of Oahu, in waters 4760 m deep; data from O. Holm-Hansen reported in

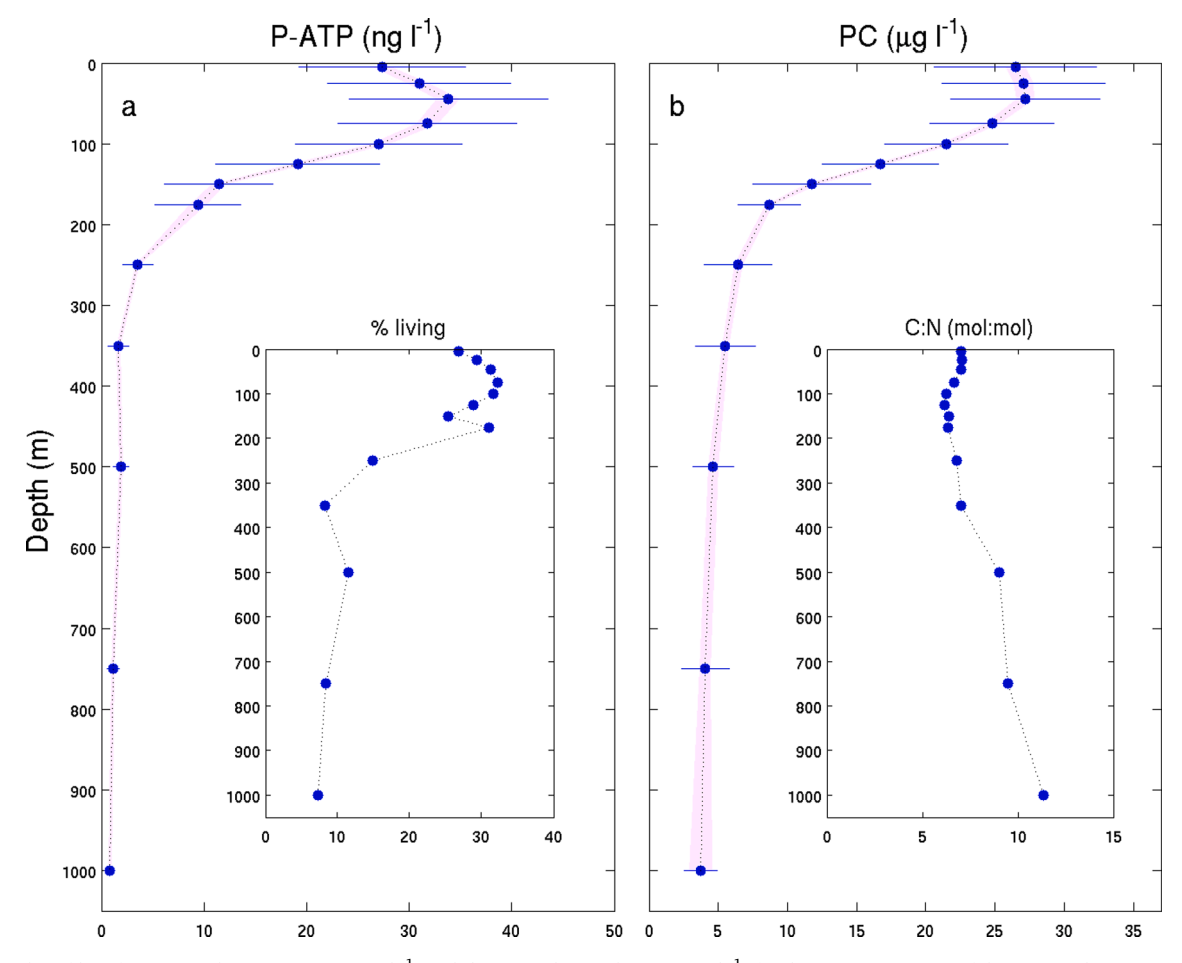


Fig. 1. Vertical profiles of (a) particulate ATP (P-ATP, ng l⁻¹) and (b) particulate carbon (PC, μ g l⁻¹) for the upper 0–1000 m of the water column at Station ALOHA. Data shown are the 30-yr mean values ± 1 standard deviation (SD) for each reference depth, along with the 95% confidence intervals (CI) in light red shading. The SD values for the 750 and 1000 m P-ATP concentrations are smaller than the size of the symbols (see Table 1 for data). Also shown as insets are: (a inset) the 30-yr mean percent living C, calculated as P-ATP \times 250 (in μ g l⁻¹) divided by PC (μ g l⁻¹) times 100%, and (b inset) is the 30-yr mean PC to particulate N (PN) molar ratio.

Table 1Particulate ATP (P-ATP) concentrations measured in the upper 0–1000 m of the water column at Station ALOHA during the period 1989–2018.

Depth	P-ATP (ng l	⁻¹)			
(m)	Mean	SD	95% CI	n	
5	27.4	8.1	26.5-28.4	278	
25	31.0	8.9	30.0-32.1	279	
45	33.9	9.7	32.7-35.0	279	
75	31.8	8.7	30.8-32.8	287	
100	27.1	8.1	26.1-28.1	290	
125	19.2	8.0	18.3-20.1	295	
150	11.5	5.3	10.8-12.1	280	
175	9.4	4.2	8.6-10.2	102	
250	3.5	1.5	3.4-3.7	276	
350	1.6	1.0	1.5-1.8	171	
500	1.9	0.8	1.8-2.1	98	
750	1.1	0.6	1.0-1.3	99	
1000	0.9	0.5	0.8-0.9	101	

Table 2Water column particulate matter concentrations and inventories of P-ATP, PC, and biomass-C at Station ALOHA.

Depth Range	P-ATP ^a		PC ^b	Biomass-C ^c	%
(m)	(ng l ⁻¹)	(mg m ⁻²)	$(g m^{-2})$	$(mg m^{-2})$	Living
0–100	31.0	3.1	2.6	775	29.8
100-250	11.3	1.7	1.7	425	25.0
250-1000	1.9	1.4	3.4	350	10.3
1000-2000	0.7	0.7	2.6	175	6.7
2000-3000	0.4	0.4	2.6	100	3.9
3000-4800	0.3	0.6	4.8	150	3.1

 $^{^{\}rm a}\,$ mean concentrations and total inventories within specified depth range.

Gordon, 1970). Even though the P-ATP concentrations are low, the deep water column (>1000 m) inventory of 1.7 mg P-ATP m $^{-2}$, equivalent to a microbial biomass of 425 mg C m $^{-2}$, is substantial (Table 2).

The 30-yr mean vertical profile of PC concentrations mostly conforms to P-ATP with maximum concentrations in the upper 0–100 m, a steep decreasing concentration gradient in the lower euphotic zone to upper mesopelagic zone transition (100–250 m), and a less steep decreasing concentration gradient from 250 to 1000 m (Fig. 1b and Table 3). Two important distinctions between the independent profiles were the lack of peaks in PC at 45 m and 500 m, as seen for the 30-yr mean P-ATP profile, and the smaller range of concentrations in the upper 0–1000 m of the water column (an 8-fold range from 3.4 to 27.2 $\mu g \ l^{-1}$ for PC versus a 38-fold range from 0.9 to 33.9 $ng \ l^{-1}$ for P-ATP; Table 1). The 0–100 m, 100–250 m, and 250–1000 m PC inventories of

2.6, 1.7, and 3.4 g C m⁻², respectively, represent a decreasing percentage of living C with increasing depth from \sim 30% in near-surface waters to <10% in the lower mesopelagic zone (Fig. 1a inset and Table 1). The less well resolved (in time) deep water observations (\geq 1000 m) indicate a continually decreasing percentage of living C to values \sim 3–4% at depths >2000 m (Table 2).

The vertical profile of PN conforms to that of PC, except for a slightly more rapid decrease of N, relative to C, below $\sim\!350$ m (Table 3). Consequently, the molar PC:PN ratios are nearly constant in the 0–350 m portion of the water column (6.2–7.1), increasing to a mean value $>\!10$ at 1000 m (Fig. 1b inset and Table 3), and to even higher values in the bathypelagic zone (Gordon, 1971).

3.2. Seasonal and interannual variations in P-ATP, PC, and PN

During the 30-yr observation period, P-ATP concentrations in the upper 0-100 m of the water column varied on seasonal and interannual time scales, but without discernible long-term trends (Fig. 2 and Tables 4 and S-1). For example, P-ATP concentrations exhibited predictable seasonality with higher than annual mean values in spring (Mar-Apr) and summer (Jul-Sep) compared to other seasons, especially at 45 m and below (Fig. 2 and Table 4). The summertime mean P-ATP concentrations were 7%, 15%, 32%, 25%, and 26% higher than the wintertime minima at 5, 25, 45, 75, and 100 m, respectively (Fig. 2 and Table S-1). The peak 0-100 m depth-integrated P-ATP inventory in Aug was \sim 0.7 mg m⁻² greater than the Feb minimum, representing a seasonal change of \sim 30–35% in biomass-C (Fig. 3a-c). Superimposed on this predictable seasonal climatology were interannual variations in the upper euphotic zone (0-100 m) P-ATP inventories of even greater magnitude than the mean seasonal fluctuations (Fig. 4a-c). For example, 1994 and 2000 stand out as years when the upper water column inventory of P-ATP was significantly higher than the 30-yr average (Fig. 4a-c). The elevated P-ATP inventories during 1994 were ~150% of the 30-yr mean.

In the lower portion of the euphotic zone (125–150 m), the seasonal peak in P-ATP concentration shifted to spring (Mar-May), with minima in fall (Sep-Nov) and winter (Dec-Feb) seasons (Table S-1). Below the euphotic zone (\geq 175 m), there was no consistent seasonal pattern in P-ATP concentrations (Table S-1). Depth-integrated P-ATP inventories inthe transition region from the lower euphotic zone to upper mesopelagic zone (100–250 m) displayed stochastic variability with no predictable seasonality (Fig. 5 and Table S-1). Below 250 m, the P-ATP was more variable, probably due to lower concentrations (Table S-1).

PC concentrations in the upper euphotic zone (0–100 m) displayed seasonal patterns with maxima in summer (Fig. 3d-f and 6, and Table S-1). A similar trend was observed for PN (data not shown). The seasonal variations (minimum to maximum seasonal values) in PC ranged from 12 to 27% depending on depth. In the lower portion of the euphotic zone (100–175 m), the peak PC concentrations shifted to the spring (Table S-

Table 3
Particulate carbon (PC) and nitrogen (PN) concentrations and PC:PN molar ratios measured in the upper 0–1000 m of the water column at Station ALOHA during the period 1989–2018.

Depth	PC (μ g l $^{-1}$)	PC (µg l ⁻¹)			PN (μ g l ⁻¹)			PC:PN (mol mol ⁻¹)		
(m)	Mean	SD	n	Mean	SD	n	Mean	SD	n	
5	26.5	5.8	289	4.5	1.0	287	7.0	1.2	287	
25	27.1	5.9	303	4.5	0.8	301	7.1	1.2	300	
45	27.2	5.4	289	4.6	0.9	284	7.0	1.2	284	
75	24.8	4.5	298	4.4	0.8	296	6.7	1.0	295	
100	21.5	4.5	318	4.1	0.9	315	6.3	1.1	315	
125	16.7	4.2	307	3.2	0.9	306	6.2	1.5	305	
150	11.8	4.3	300	2.2	0.7	298	6.4	1.3	298	
175	8.7	2.3	282	1.6	0.4	282	6.4	1.1	281	
250	6.4	2.5	273	1.1	0.4	271	6.8	1.8	270	
350	5.5	2.2	340	0.9	0.3	338	7.0	1.3	338	
500	4.6	1.5	78	0.7	0.3	77	9.0	4.5	77	
750	4.1	1.7	83	0.6	0.3	84	9.5	5.4	83	
1000	3.4	1.3	76	0.5	0.2	77	10.8	10.3	76	

b lower mesopelagic/bathypelagic (>1000 m) PC data from Gordon (1971).

^c biomass-C inventory in specified depth range assuming a biomass-C:ATP ratio of 250:1 (see text for details).

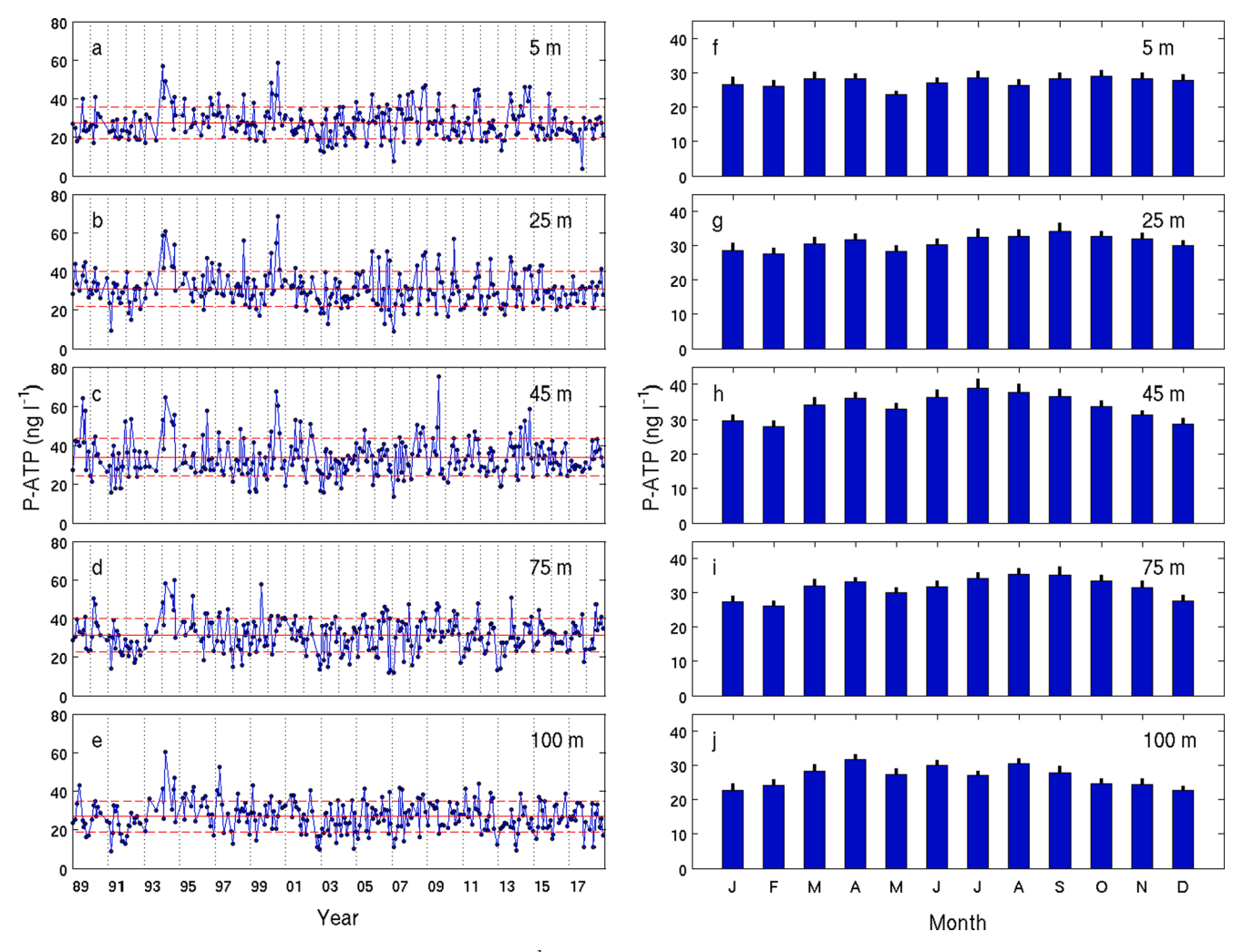


Fig. 2. (a-e) Time-series (1989–2018) of particulate ATP (P-ATP, $ng l^{-1}$) at five reference depths in the upper euphotic zone (0–100 m) at Station ALOHA. Shown in blue symbols are the values for each of the 278–290 sampling dates, along with the mean (solid red line) ± 1 standard deviation (dashed red lines) values (see Table 1 for data). (f-j) Monthly climatologies for P-ATP ($ng l^{-1}$) for each reference depth presented as mean and +1 standard deviation based on the 30-yr time series.

Table 4Contributions to the observed time-series (1989–2018) variance by the climatological seasonal cycle, interannual variability, and long-term linear trend. The subseasonal contribution is estimated as the residual variance once the seasonal, interannual, and long-term components have been subtracted from the total variance.

	Depth	% variability					
Parameter	(m)	Seasonal Interannual		Long-term Trend	Sub- seasonal		
P-ATP	5	1.4	26.0	0.7	72.0		
	25	4.9	23.0	1.3	70.8		
	45	11.1	19.9	0.2	68.8		
	75	9.9	21.6	0.1	68.5		
	100	9.5	21.7	0.6	68.2		
	125	16.8	17.8	2.6	62.8		
	150	13.7	18.4	2.6	65.3		
	250	2.9	36.7	17.8	42.6		
PC	5	23.9	10.9	1.7	63.4		
	25	22.3	11.0	0.2	66.5		
	45	28.4	13.9	3.9	53.7		
	75	23.7	19.7	4.4	52.3		
	100	7.9	18.8	0.7	72.6		
	125	24.1	11.9	0.3	63.7		
	150	19.1	12.8	2.8	65.2		
	250	8.7	16.9	2.3	72.1		

1), a pattern that is identical to the pattern observed for P-ATP. At depths >175 m, no consistent seasonal patterns were observed for PC concentrations (Table S-1). There was no seasonality for the PC:PN molar ratios at any depth (data not shown). The 0-100 m depthintegrated inventories for PC increased in late summer and remained high through Oct, compared to the much shorter, summer-only peak in P-ATP (Fig. 3e,f). Furthermore, PC was elevated throughout the upper 0-75 m of the water column, compared to the peak P-ATP concentration centered at 45 m (Fig. 3 and Table S-1). The 0-100 m depth-integrated PC displayed substantial interannual variability with 2010 and 2016 standing out as higher than average years and 1990, 1994, and 1996 representing lower than average years (Fig. 7). These years of anomalously high and low PC inventories in the upper euphotic zone (0-100 m), relative to the 30-yr mean, do not align with the interannual patterns for P-ATP (compare Fig. 4c and 7c), suggesting control by independent mechanisms. Consequently, the biomass-C (P-ATP \times 250):PC ratios displayed stochastic variability on both seasonal and interannual time scales (Fig. 8). Finally, the cumulative percentage plots for biomass-C and total PC display distinct patterns with a much higher percentage of biomass-C in the upper region of the water column (Fig. 1a inset and Fig. 9).

4. Discussion

It is difficult to overstate the ecological significance of the ATP-

biomass method when it was introduced in 1966, and its continuing relevance today (Henderikx-Freitas et al., 2021; Bochdansky et al., 2021). In 1966, there was no reliable procedure to measure total living carbon in aquatic ecosystems. The best approach at that time was the Utermöhl method that involved the settling of organisms by gravity, followed by inverted microscopic enumeration and biovolume estimation (Utermöhl, 1931; Lund et al., 1958). A biovolume-to-cell C conversion factor was then applied to estimate total biomass. This method was limited to microorganisms larger than \sim 2 μm , including eukaryotic algae, heterotrophic protists, and micrometazoans (Beers et al., 1975). In 1966, the enumeration of bacteria relied on either microscopic or culture techniques, but quantitative comparisons of the two methods revealed large disparities of several orders of magnitude (Jannasch and Jones, 1959, recently reviewed by Williams and Ducklow, 2019). Even after dye-based epifluorescence microscopic methods were accepted as the most accurate approach, questions remained about the distinction between live versus dead cells, and the propagation of errors in converting cell numbers to biovolume to biomass-C, over some specified depth interval (Newell et al., 1986). Because microbes generally represent the largest pool of living organic matter in the sea, microbial biomass estimation is important for food web modeling and related ecological studies. However, accurate estimation of total microbial biomass is challenging because microbes in the sea vary considerably in size from $\sim 0.2~\mu m$ to 200 μm and because their size overlaps with particulate organic detrital materials (Sieburth et al., 1978). The ATPbiomass assay offered a relatively objective and sensitive crossphylogenetic domain method that could be universally applied to all

trophic classes for estimates of total microbial biomass. Furthermore, when used in conjunction with membrane filter size separation, the ATP-biomass method could obtain size spectra of microbial biomass in a given habitat. Even today, more than half a century after Holm-Hansen and Booth's (1966) benchmark paper, it represents one of the most reliable methods for total microbial biomass determination.

To our knowledge, these observations from Station ALOHA (also see Winn et al., 1995; Björkman and Karl, 2005 for additional Station ALOHA data summaries) are the first multi-year study of P-ATP in the sea, with the possible exception of the Food Chain Research Group's 6 cruise, 18-month time series in the Southern California Bight (Eppley et al., 1977). P-ATP has been measured in several previous studies of the NPSG, including a single profile at Station Gollum in Jun 1970 (Holm-Hansen and Paerl, 1972), as well as measurements in the euphotic zone on several expeditions within the Climax study region (26-28°N, 155°W; Eppley et al., 1973; Beers et al., 1975; Perry and Eppley, 1981; Jones et al., 1996; Björkman et al., 2000) and a single deep water profile in Jun 1977 (Williams et al., 1980). However, there is no information on temporal variability of P-ATP for any region of the world oceans, or on the dynamics of the depth-dependent relationships between living versus nonliving particulate organic matter. A previous analysis of the Station ALOHA time series (1989-1993) reported weak P-ATP seasonality in the lower portion of the euphotic zone (100-175 m) with peak concentrations in mid-Apr (Winn et al., 1995). Because the peak in the lower euphotic zone corresponded to a springtime increase in Chl a and primary production, the authors concluded that the seasonal increase in irradiance led to the net growth of phytoplankton (Winn et al., 1995).

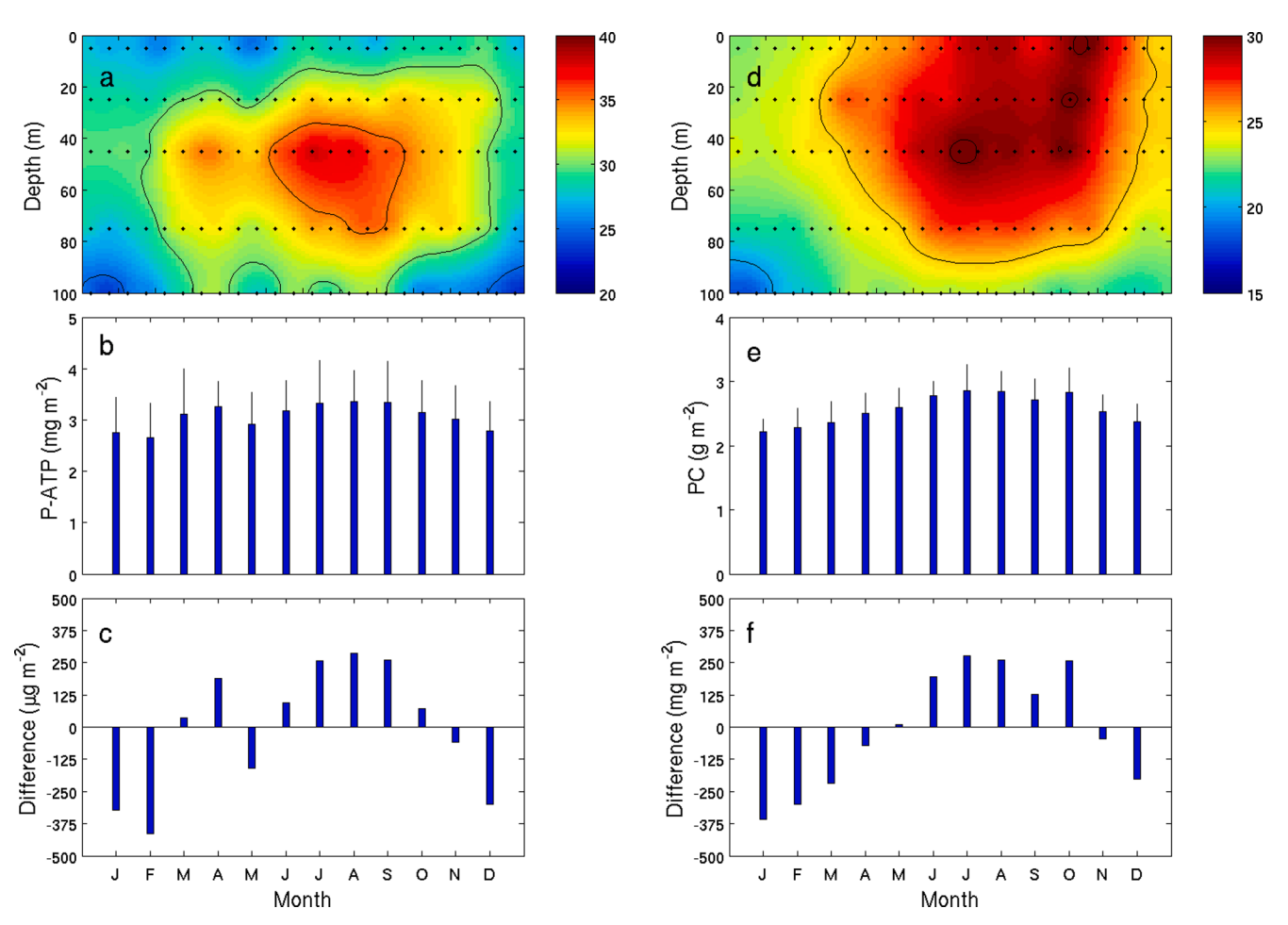


Fig. 3. (a, d) Contour plots of the monthly climatologies of particulate ATP (P-ATP, ng l^{-1}) and particulate carbon (PC, μ g l^{-1}) concentrations at Station ALOHA. Contour intervals are 5 ng ATP l^{-1} and 5 μ g PC l^{-1} , respectively. Also shown (b, e) are the monthly climatologies for the 0–100 m depth-integrated inventories of P-ATP (mg m $^{-2}$) and PC (g m $^{-2}$) as mean +1 standard deviation, and (c, f) the signed difference for each parameter and each month (μ g m $^{-2}$ and mg m $^{-2}$, respectively, from the 30-yr mean values.

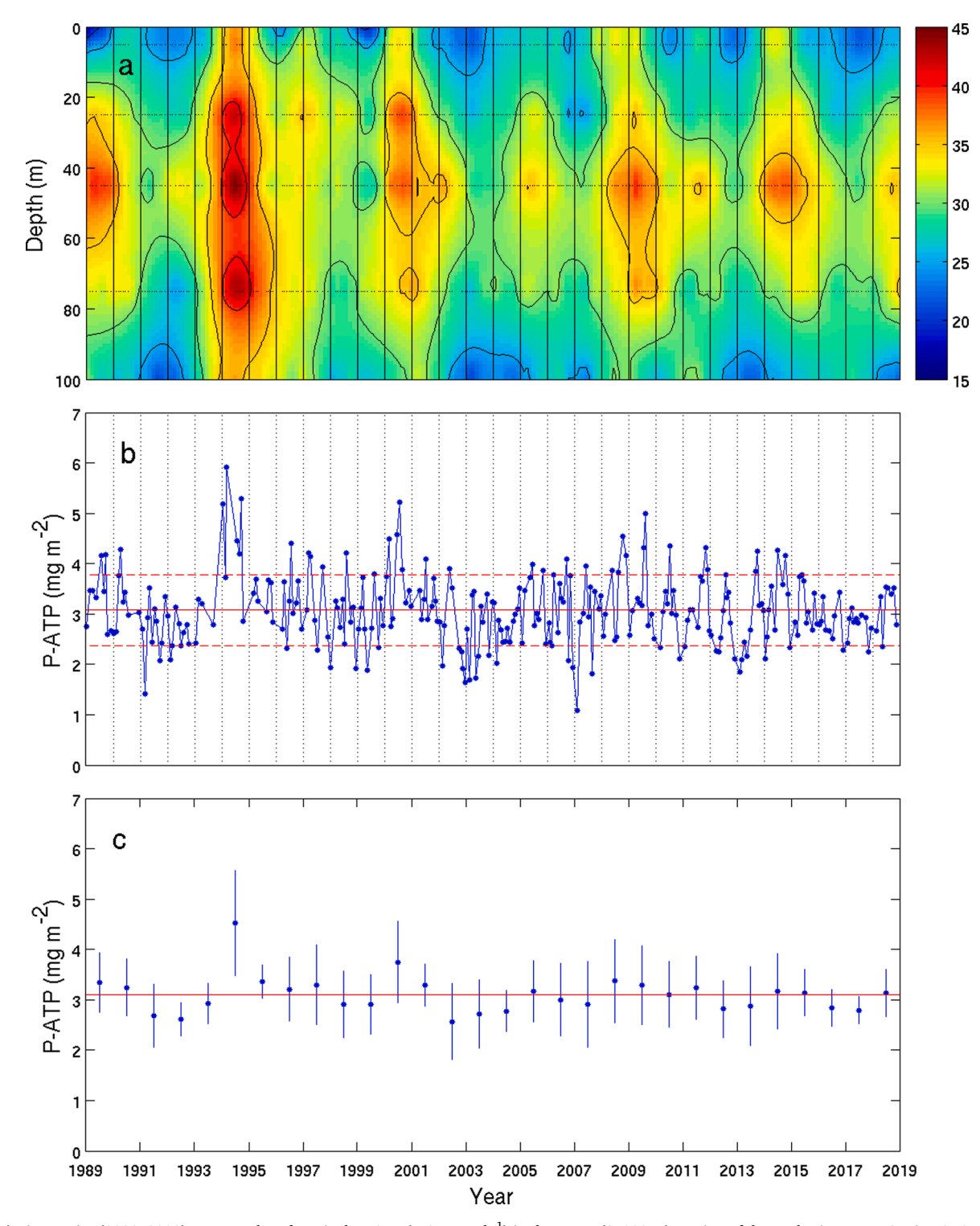


Fig. 4. (a) Time-series (1989–2018) contour plot of particulate ATP (P-ATP, ng I^{-1}) in the upper (0–100 m) portion of the euphotic zone at Station ALOHA. Contour interval is 5 ng P-ATP I^{-1} . (b) Time-series of 0–100 m depth-integrated particulate ATP (P-ATP, mg I^{-2}) showing values for each of the 277 sampling dates as well as the 30-yr mean (solid red line) and ± 1 standard deviation (dashed red lines) values (see text for data). The standard deviation for each cruise integral is within the size of the symbol. (c) Annually averaged 0–100 m depth-integrated P-ATP inventories (mg I^{-2}) showing the mean I^{-2} standard deviation for each year. The horizontal red line is the 30-yr mean value of 3.1 mg ATP I^{-2} .

Letelier et al. (2004) subsequently documented the inextricable linkages among light, nutrients, and phytoplankton biomass in the lower euphotic zone at Station ALOHA. The more comprehensive P-ATP time series presented herein confirms these seasonal dynamics of P-ATP in the lower portion of the euphotic zone.

The seasonality of P-ATP and PC with depth derived from the present

30-year record reveals distinct temporal patterns (Fig. 10). Whereas the seasonal amplitude of P-ATP in surface waters (5 and 25 m) is relatively modest (10–20%) with increases in late summer to early fall (Figs. 3 and 10a), the concentrations of P-ATP in the lower portion of the euphotic zone (125 and 150 m) display peak amplitudes in spring that are \sim 70% greater than the seasonal minima at those depths. This near doubling of

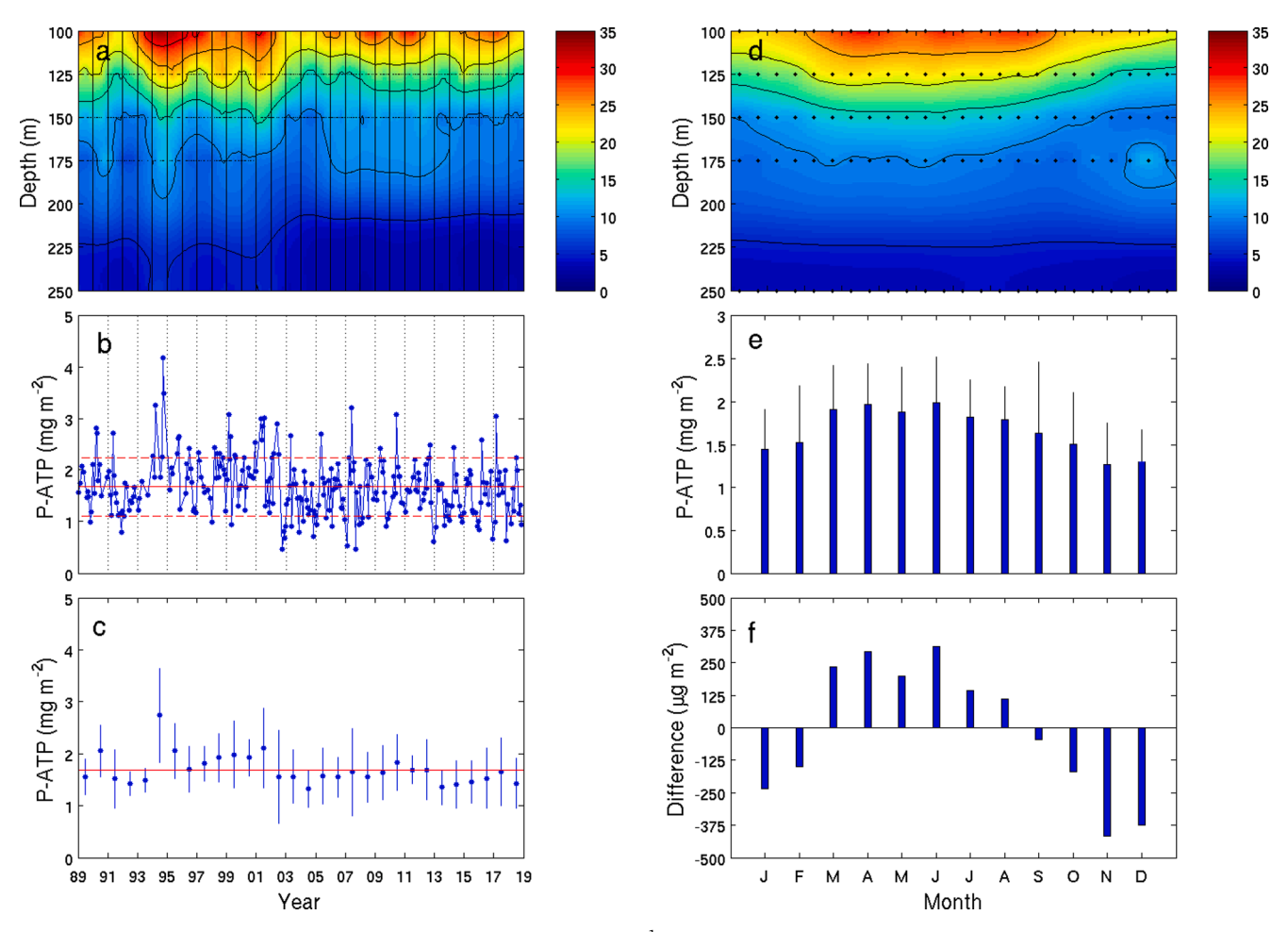


Fig. 5. (a) Time-series (1989–2018) contour plot of particulate ATP (P-ATP, ng l⁻¹) concentrations for the lower portion of the euphotic zone and upper portion of the mesopelagic zone (100–250 m) at Station ALOHA. Contour interval is 5 ng P-ATP l⁻¹. (b) Time-series (1989–2018) of the 100–250 m depth-integrated P-ATP inventories (mg P-ATP m⁻²) showing the mean (1.68 mg P-ATP l⁻¹, solid red line) and ± 1 standard deviation (SD = 0.57 mg P-ATP l⁻¹, dashed red lines) for the 30-yr observation period (n = 277). (c) Annually averaged 100–250 m depth-integrated P-ATP inventories (mg m⁻²) showing the mean ± 1 SD for each year. The horizontal red line is the 30-yr mean value of 1.68 mg P-ATP l⁻¹. (d) Contour plot of the monthly climatologies for P-ATP (ng l⁻¹) for the 100–250 m portion of the water column. Contour interval is 5 ng P-ATP l⁻¹. (e) Monthly mean ± 1 SD values for the 100–250 m depth-integrated P-ATP inventories (mg m⁻²). (f) Signed differences from the 0–100 m depth-integrated P-ATP inventory (µg P-ATP m⁻²) for each month from the annual mean inventory value of 1.68 mg P-ATP m⁻².

the microbial biomass at those lower euphotic zone depths is consistent with a spring bloom of phytoplankton sustained by the wintertime buildup of nutrients due to light limitation (Letelier et al., 2004). The peak P-ATP concentrations (≥60% seasonal increase) are relatively short-lived (<3 months), presumably due to the assimilation of accumulated nutrients. In contrast to these seasonal patterns in P-ATP, suspended PC at both 25 m and 125 m accumulates from seasonal minima in winter to peak values in summer (125 m) and fall (25 m). At both reference depths, there is a large seasonal accumulation of nonliving PC (difference between PC and P-ATP × 250; Figs. 3 and 10b,c). For example, the seasonal PC accumulation in surface waters (25 m) is 4.5 times as large as that derived from P-ATP, assuming a C:ATP ratio of 250, and 2.5 times at 125 m (Fig. 10b,c). These dynamics of biomass-C and detrital C document a seasonal build-up of nonliving PC throughout most of the year, consistent with shorter residence times for P-ATP than PC at Station ALOHA. However, each winter the system resets to minimum values for each parameter, as a result of net loss of biomass, and remineralization and export of nonliving particulate organic matter. Indeed, Hebel and Karl (2001) have previously reported seasonal changes in the C-N-P elemental composition of suspended particulate matter, specifically significant changes in the bulk elemental composition and a return to a near Redfield stoichiometry of the particulate matter pool each winter.

Karl et al. (2021) recently reported a long-term increasing trend in

 $^{14}\text{C-based}$ primary production at Station ALOHA for the period 1989–2018. The 0–125 m depth-integrated trend of 4.0 mg C m $^{-2}$ yr $^{-1}$ had the largest relative increase (37%) in the lower portion (75–125 m) of the euphotic zone (Karl et al., 2021). They also reported significant, but lower, relative increases in PC (17%), PN (8%), and Chl a (8%) in the lower portion of the euphotic zone since 1989. We evaluated the 30-yr time series for P-ATP at 75, 100, and 125 m, as well as the 75–125 m depth-integrated P-ATP inventory and observed only at 125 m a significant long-term decreasing trend in P-ATP (-0.15 ng l $^{-1}$ yr $^{-1}$, 95% confidence interval $=\pm0.11$).

The mean vertical profile of P-ATP at Station ALOHA displays a range of 50-fold from values of $\sim\!\!34$ ng l^{-1} at 45 m to $<\!\!0.7$ ng l^{-1} in the bathypelagic zone (Fig. 1a and Table 2). Assuming a constant microbial C:ATP ratio of 250:1 (Holm-Hansen, 1973; Karl, 1980), the distribution of total living C ranges from a maximum of 8.3 µg l^{-1} in the upper euphotic zone to $\sim\!\!0.1\!-\!0.2\,\mu g\,l^{-1}$ at great ocean depths. These estimates of living C represent a decreasing proportion of the total PC. The dominance of nonliving particulate organic detritus throughout the water column in all seasons is confirmed by the 30-yr time-series of P-ATP and PC at Station ALOHA reported herein.

Based on the mean P-ATP profile, we have divided the water column into four distinct regions: upper euphotic zone (0–100 m), lower euphotic-to-upper mesopelagic zone transition (100–500 m), mesopelagic zone (500–1000 m), and bathypelagic zone (>1000 m). Unique

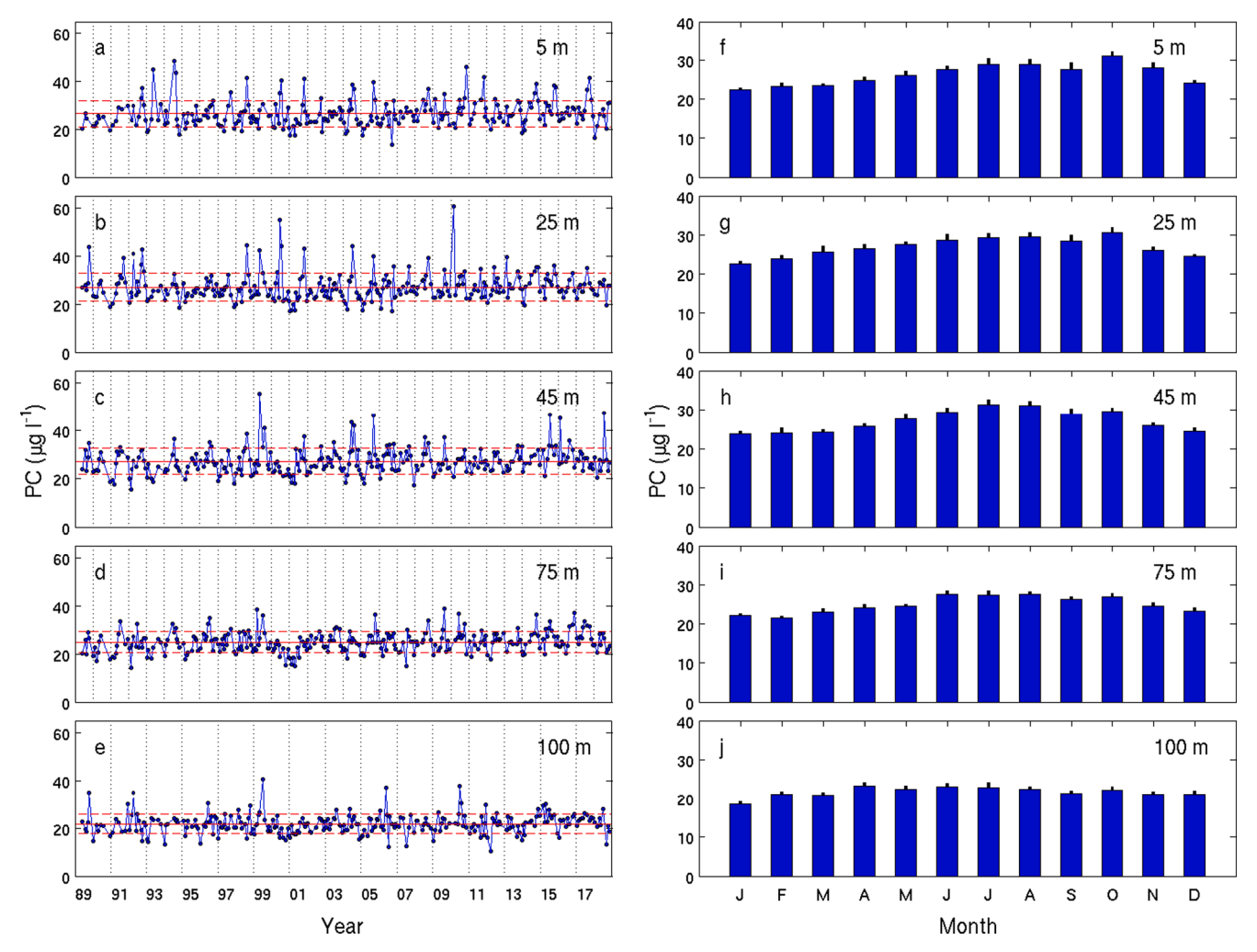


Fig. 6. (a-e) Time-series (1989–2018) and (f-j) monthly climatologies presented exactly as in Fig. 2, except as particulate C (PC, μ g l⁻¹) concentrations.

features of each region are presented below.

4.1. Microbial biomass depth distributions and organism attributions: upper euphotic zone

As expected, the upper portion of the euphotic zone had the highest P-ATP concentrations. There are several notable features in the 30-yr time series including: (1) a significant seasonal variability with peak P-ATP observed in summer, (2) near uniform P-ATP concentrations with depth, but with a distinct, permanent peak at 45 m, and (3) a significant interannual variability with annual mean values for 1994 and 2000 standing out as years with higher than average P-ATP inventories (\sim 43% and 20% higher, respectively), and 1992 and 2003 standing out as years with lower than average P-ATP inventories (both \sim 15% lower; Fig. 4).

The mean P-ATP inventory for the upper 0–100 m region of the water column was 3.1 (SD = 0.7 mg m $^{-2}$, n = 277), which equates to a total microbial biomass of 775 mg C m $^{-2}$ or an average of 7.8 µg C l $^{-1}$ for the upper euphotic zone. We expect that photoautotrophs, including both picocyanobacteria and eukaryotic algae, would comprise a substantial fraction of biomass-C in the upper euphotic zone, so it is imperative to have an accurate C:ATP ratio for representative marine phytoplankton. While numerous laboratory studies have examined the C:ATP ratio in marine algae growing under a variety of physiological conditions (Holm-Hansen, 1973; Sakshaug and Holm-Hansen, 1977; Laws et al., 1983), there are limited field data from natural phytoplankton assemblages. Eppley et al. (1971) performed a series of nutrient enrichment growth experiments off southern California to constrain phytoplankton

community composition, including PC, PN, Chl a, and P-ATP. By tracking increases in the composition of total particulate matter over a period of several days following fixed nitrogen amendments (nitrate, ammonium, or urea), they were able to estimate the average elemental stoichiometry and C:ATP ratios of newly synthesized phytoplankton biomass. For the six separate shipboard experiments that were conducted, the mean C:ATP was 265 (range 230-290), a value that is similar to that of nutrient-replete growth of unialgal cultures in the laboratory (e.g., Laws et al., 1983). A recent, yet unpublished, study of Prochlorococcus (strain MED4), the most abundant photoautotroph at Station ALOHA, has also confirmed a similar C:ATP ratio under nutrientreplete conditions (D. Lindell, K. Björkman, and others, unpublished data). Consequently, the use of a C:ATP ratio of 250 for the upper euphotic zone at Station ALOHA is justified, and the 7.8 $\mu g \; C \, l^{-1}$ average biomass-C probably sets an upper limit for the total phytoplankton assemblage.

Jones et al. (1996) used the 14 C-incorporation into Chl a method (Laws, 1984) to estimate phytoplankton-C in the euphotic zone in the Climax region. Their derived phytoplankton C:Chl a ratio (g g $^{-1}$) was 156 for the upper 0–80 m of the water column, and was similar to the value of 128 ± 10 g g $^{-1}$ reported by Campbell et al. (1994), but higher than the value of ~ 100 (range 90–112) measured by Eppley et al. (1971) in their shipboard culture experiments. Jones et al. (1996) reported an average biomass of 8.2 ± 0.75 µg C l $^{-1}$ for upper (0–100 m) euphotic zone phytoplankton, compared to PC concentrations ranging from 30 to 42 µg C l $^{-1}$, higher than the mean PC value of ~ 27 µg C l $^{-1}$ for Station ALOHA. Based on their analysis, phytoplankton-C accounted for

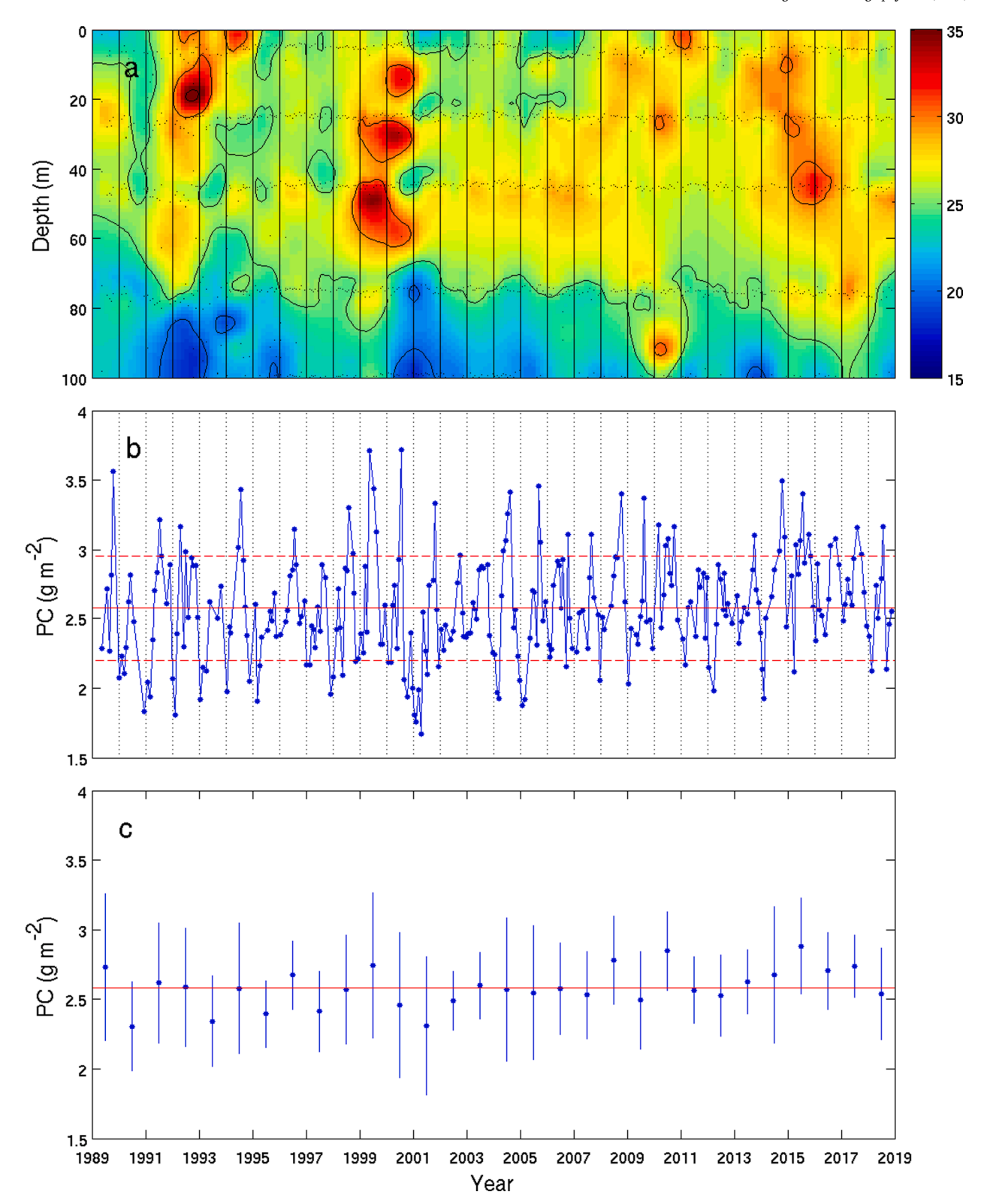


Fig. 7. (a) Time-series (1989–2018) contour plot of PC ($\mu g \, \Gamma^1$), (b) 0–100 m depth-integrated inventories, and (c) annually averaged 0–100 m depth-integrated mean value (2.6 mg m⁻²) presented exactly as in Fig. 4, except as particulate carbon (PC, g m⁻²). Contour interval in (a) is 5 $\mu g \, PC \, \Gamma^{-1}$.

$\sim\!20\text{--}27\%$ of the total PC (Jones et al., 1996).

Several previous studies in the NPSG have estimated total microbial biomass using a variety of microscopic methods, flow cytometry, and extrapolation of cell abundances and biovolume estimates to biomass-C (Table S-2). The accuracy of these methods depends on the value, or values, used for the biovolume-to-biomass conversion, much in the same

way as the extrapolation of P-ATP concentrations depends on the accuracy of the C:ATP ratio. A broad range of published (and therefore "acceptable") values have been used for this purpose (Strathmann, 1967; Verity et al., 1992; Christian and Karl, 1994; Menden-Deuer and Lessard, 2000; Worden et al., 2004; Casey et al., 2013). For example, literature estimates of the per cell C quota for *Prochlorococcus* range from

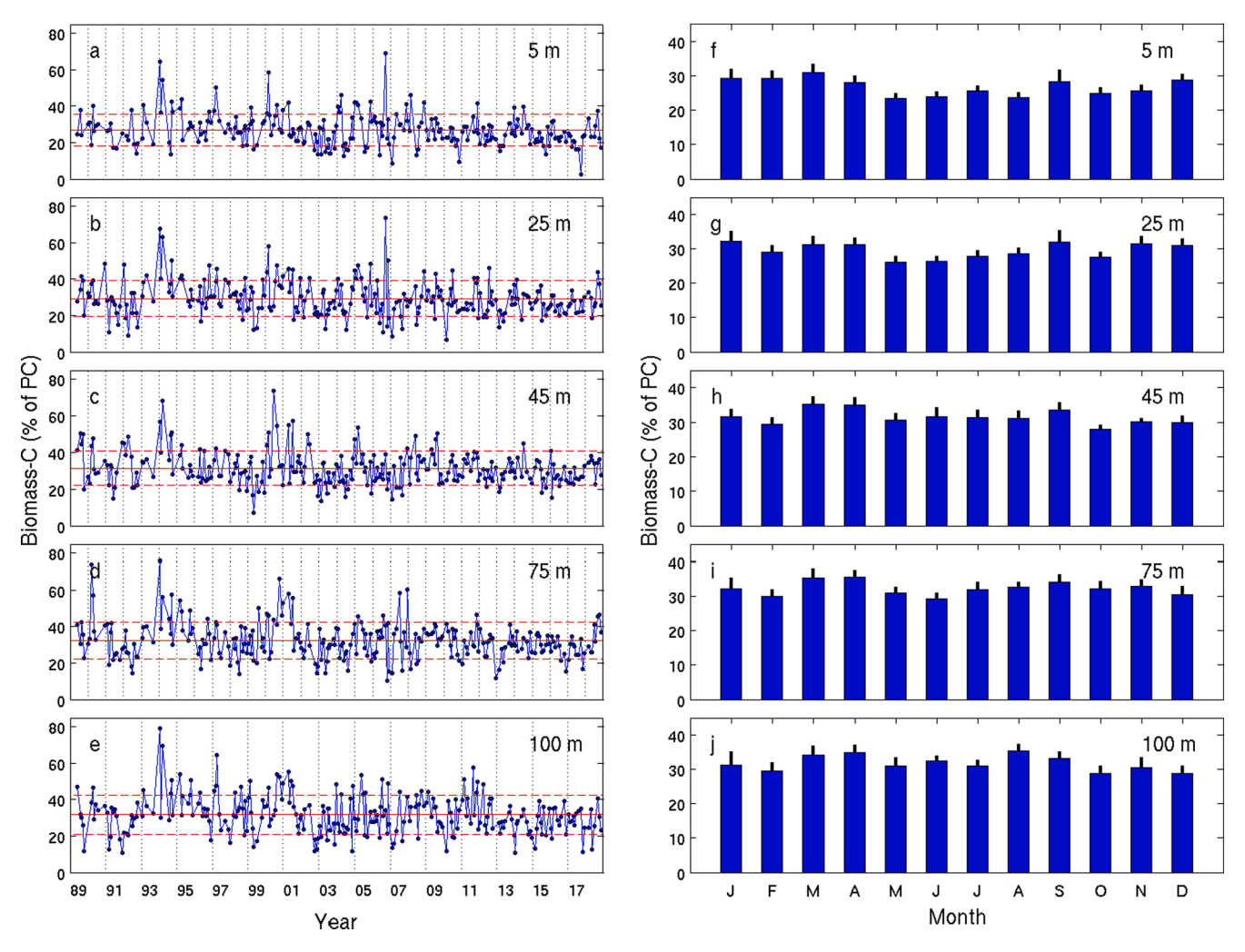


Fig. 8. (a-e) Time-series (1989–2018) and (f-j) monthly climatologies presented exactly as in Fig. 2, except as Biomass-carbon (C) shown as a percentage of total particulate carbon (PC).

<10 fg C cell⁻¹ to >150 fg C cell⁻¹ (Casey et al., 2013). Some of this variability is probably real based on expected changes in cell size due to growth rate, timing of the cell cycle, nutrition, and other culture variables. For the most accurate per cell C quota estimates, it is imperative to determine cell biovolume (rather than abundance), since the C content per unit biovolume (i.e., the C density) decreases significantly with increasing cell volume (Menden-Deuer and Lessard, 2000; Segura-Noguera et al., 2016).

In a comprehensive study of the Climax region (expedition TASADAY-I, Jun 1973), Beers et al. (1975) measured microplankton (2–200 µm) by the Utermöhl method, P-ATP, and PC concentrations at 6 stations covering an approximately 32 km × 32 km grid to assess small scale spatial variability (although the sampling was not synoptic). To estimate microplankton cell volume, they measured two dimensions and estimated the third using shape analysis, then applied the biovolume-tobiomass relationship of Strathmann (1967) to derive total cell C. By this analysis, microplankton biomass-C in the upper 0-80 m of the water column was reported to be ${\sim}8~\mu g~C~l^{-1},$ equivalent to 32% and 30% of the total PC for depth intervals of 0-20 m and 40-80 m, respectively (Beers et al., 1975; Table S-2, row #1). They concluded that the dominant fraction of the total PC was either detritus or living microorganisms less than their lower detection of 2 µm, though they suspected the former (Beers et al., 1975). By comparison, their P-ATP based estimate of mean biomass-C in the upper 0–100 m of the water column was $19.8 \mu g C l^{-1}$ (Table S-2, row #2). This estimate was 70-85% of the total PC, a value 2fold greater than we observe at Station ALOHA for the upper portion of

the euphotic zone (Table 2). For the 6 stations that were sampled (Beers et al., 1975), P-ATP in the 0-100 m region of the water column averaged 79 ng l^{-1} (range 61–97 ng l^{-1}), values that greatly exceed our 30-yr mean observations at Station ALOHA (Figs. 1, 3, and 4), or any previous measurements in the Climax region (Eppley et al., 1973; Perry and Eppley, 1981; Jones et al., 1996; Björkman et al., 2000), for reasons that are not known. During the 30-yr observation period at Station ALOHA, we recorded only 8 individual P-ATP measurements out of a total of 1376 (0.6%) that exceeded 60 ng l^{-1} and none exceeded 75 ng l^{-1} . Despite these anomalously elevated P-ATP concentrations in the euphotic zone, the vertical distribution pattern reported by Beers et al. (1975) indicating comparable near-surface (5 m) and 100 m concentrations (61 ng l^{-1} and 67 ng l^{-1} , respectively) and a mid-euphotic zone P-ATP peak (95 ng l^{-1} at 40 m and 97 ng l^{-1} at 60 m), are similar to the patterns that we report for Station ALOHA. In contrast to these "elevated" P-ATP concentrations (relative to all previous NPSG observations), Beers et al. (1975) reported PC concentrations for the upper 0-100 m of the water column (22–26 μ g C l⁻¹) that conform to those measured at Station Gollum (Gordon, 1971) and Station ALOHA (Hebel and Karl, 2001; Fig. 1b and Table 3), which makes their anomalously high P-ATP values that much more enigmatic. They also reported Chl a values of $0.04-0.05 \mu g l^{-1}$ in the upper euphotic zone, and surface light transmission of 0.6% at 115 m (Beers et al., 1975), both of which are similar to summertime conditions at Station ALOHA (Letelier et al., 1996, 2004), with no evidence for the presence of a surface phytoplankton bloom that sometimes occurs in the NPSG in summer (Dore

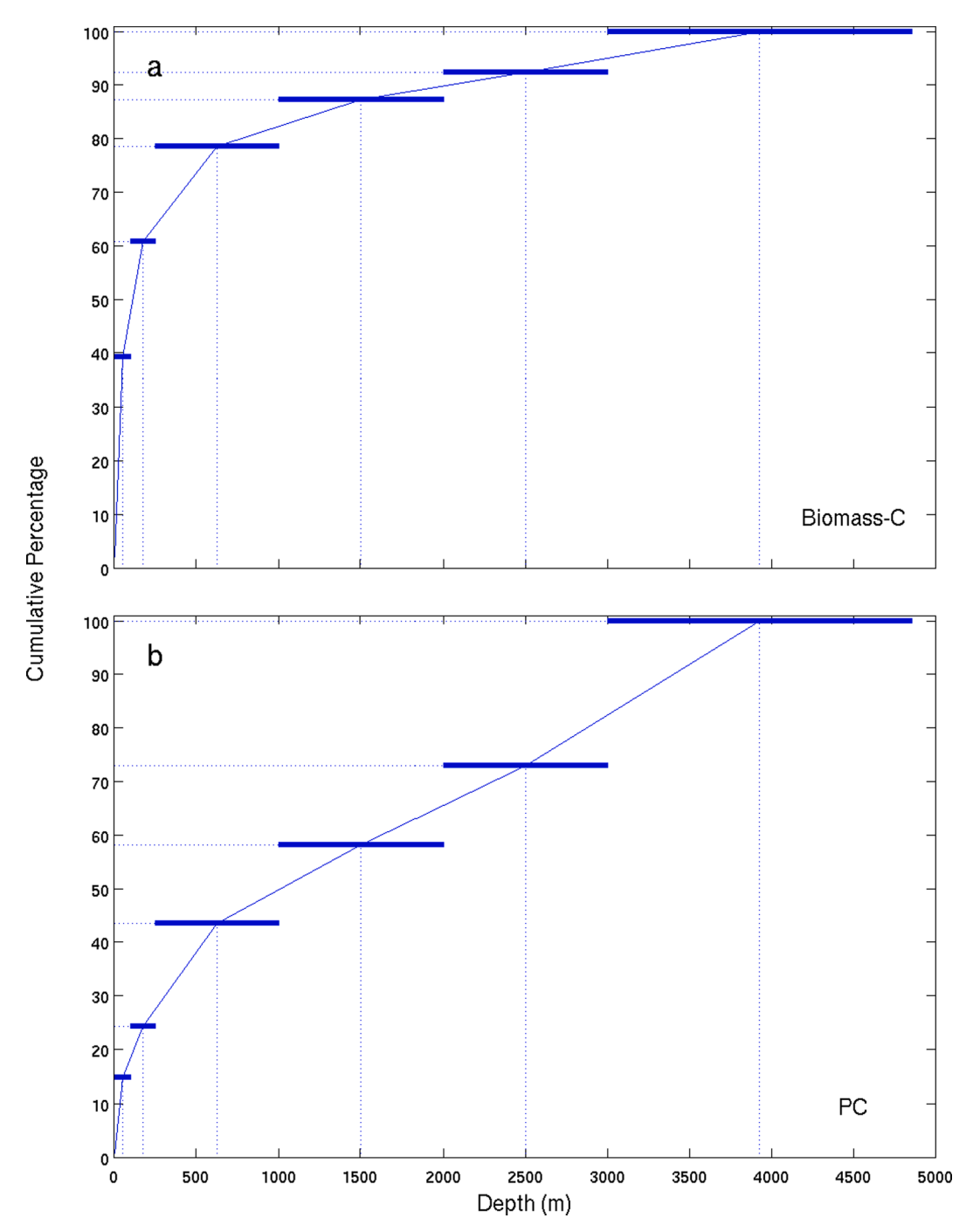


Fig. 9. Cumulative percentage plots of (a) Biomass-Carbon (Biomass-C calculated as P-ATP \times 250) and (b) particulate carbon (PC) inventories for the full water column (0–4800 m) at Station ALOHA. The horizontal bars indicate the depth range over which each parameter was integrated. The 100% inventory values are 2.0 g m⁻² for Biomass-C and 17.7 g m⁻² for PC.

et al., 2008). As a technical matter, the elevated P-ATP concentrations reported by Beers et al. (1975) might be the result of their use of integrated light emission in the ATP firefly bioluminescence reaction, which also detects other nucleotide triphosphates (e.g., guanosine triphosphate, GTP) in addition to ATP, rather than peak height of light emission that has been used by others (Jones et al., 1996; Björkman et al., 2000; this study). Karl (1978) demonstrated that use of integrated light emission can overestimate P-ATP by >100% in surface ocean waters, and Björkman and Karl (2005) have reported elevated near-surface (0–100 m) P-GTP:P-ATP ratios in early summer at Station ALOHA, so the P-ATP values reported by Beers et al. (1975) may have been systematically overestimated. Ironically, in a subsequent study of the

Climax region using the peak height method for P-ATP analysis, Williams et al. (1980) reported upper euphotic zone P-ATP concentrations that were significantly lower (\sim 3.5–6 ng l⁻¹) than we report herein for Station ALOHA, although the total adenylate (ATP + ADP + AMP) concentrations were much higher (20–50 ng l⁻¹), indicating a probable conversion from ATP to ADP and AMP due to stresses imposed on sampling or sample processing (so-called "filtration artifact"; see Karl and Holm-Hansen, 1978).

A follow-on study by Beers et al. (1982) also reported microscopically-derived microplankton biomass-C from 19 stations during 4 additional cruises to the Climax region conducted in all seasons (Table S-2, row #3), but presented no additional P-ATP data.

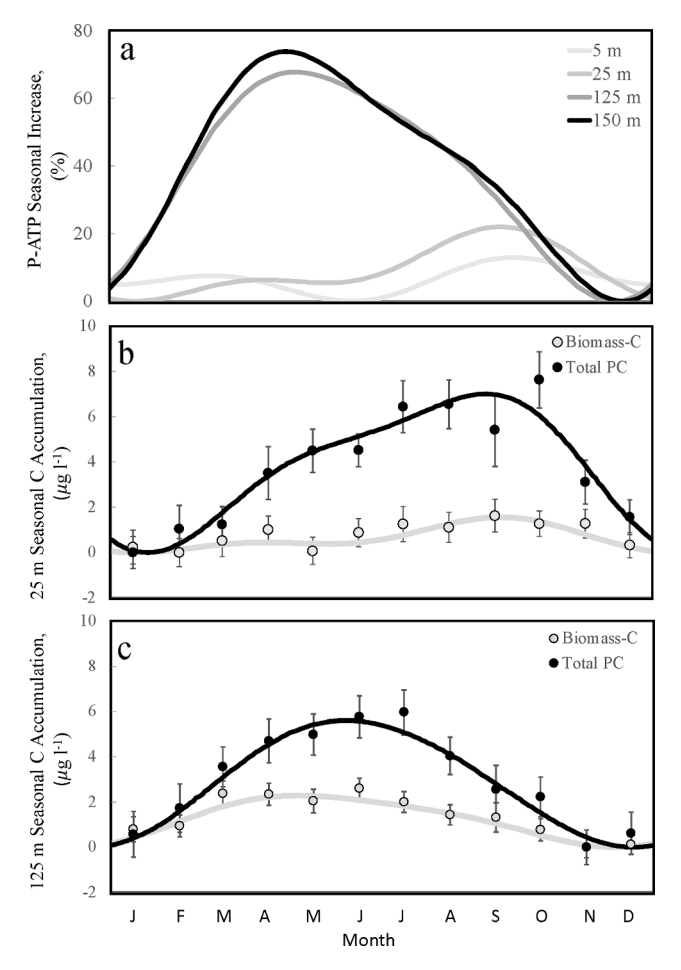


Fig. 10. Seasonal increases in total PC and P-ATP from third-order harmonic fits (lines) and monthly means ± 1 standard error (circles) derived from the 1989–2018 time-series; (a) Seasonal percentage increase of P-ATP relative to seasonal minima in the upper (5 and 25 m) and lower (125 and 150 m) euphotic zone; (b and c) Seasonal accumulation of total PC (black) and biomass-C (ATP \times 250; grey) observed at 25 and 125 m, respectively.

Microplankton biomass-C in the upper 0–80 m portion of the water column varied from $\sim\!\!7~\mu g$ C l^{-1} in late winter to $\sim\!\!10~\mu g$ C l^{-1} in late summer (Table S-2, row #3), and was always dominated by small (<5 μm) size classes. "Monads and flagellates" and non-thecate dinoflagellates were the dominant taxonomic groups representing 34–49% and 26–31% of the total microplankton biomass, respectively (Beers et al., 1982). Coccolithophorids ($\sim\!\!5\%$), thecate dinoflagellates ($\sim\!\!5\%$), and diatoms (1–3%) were relatively minor constituents.

Björkman et al. (2000) also reported microbial biomass estimates from surface waters (only) of the Climax region in summers of 1996 and 1997. They reported P-ATP (peak height of light emission)-based total microbial biomass-C values of 8.7–9.1 μ g C l⁻¹, and flow cytometric-based estimates of 13.8 (1996) and 12.5 (1997) μ g C l⁻¹, assuming C cell quotas of 10 fg, 30 fg, 100 fg, and 495 fg C cell⁻¹ for non-pigmented prokaryotes, *Prochlorococcus*, *Synechococcus*, and picoeukaryotes, respectively (Björkman et al., 2000; Table S-2, rows #4 and #5).

Laws et al. (1984) reported the initial results of the Plankton Rate Processes in Oligotrophic Oceans project (PRPOOS; Eppley, 1982) wherein a variety of methods were employed to constrain microbial biomass and growth rate. At two coastal stations off Oahu, Hawaii, the estimated biomass-C for the sum of picoplankton (0.2–2 μm ; bacteria plus cyanobacteria) plus nanoplankton (2–20 μm), both determined using microscopic techniques and a common biovolume-to-biomass C conversion of 0.15 g C ml $^{-1}$, were nearly identical to those derived from contemporaneous P-ATP measurements assuming a C:ATP ratio of 250:1

(Laws et al., 1984). At their most offshore station (Sta. F, $21^{\circ}22'N$, $158^{\circ}53'W$), the microscopically derived phytoplankton and heterotrophic nanoplankton biomass-C estimates of 5.8 and 5.5 μ g C 1^{-1} , respectively (Table S-2, row #6), compared favorably with the P-ATP derived total microbial biomass (which would also include heterotrophic bacteria) of 13.8 (SD = 3.0) μ g C 1^{-1} . Based on the reported PC for Sta. F, 34.3 μ g C 1^{-1} , the majority of the PC pool (~60%) was detritus, consistent with the results reported herein for the more oligotrophic Station ALOHA (surface PC = 23-28 μ g C 1^{-1} ; Hebel and Karl, 2001; Fig. 1b and Table 3).

One of the more comprehensive studies of microbial biomass in the sea was the project WEST-COSMIC (Western Pacific CO2 Ocean Sequestration for Mitigation of Climate Change) conducted during 1997-2001. Samples for microbial biomass were collected from the surface ocean to the abyss (up to 5800 m) along a transect from the subarctic to the subtropical biome (Yamaguchi et al., 2002, 2004; Table S-2, row #7). Several different methods were employed to enumerate and size plankton over a range of 4 orders of magnitude (0.2–2000 µm) to determine biovolumes and to estimate biomass-C (Table S-2, row #7). For the subtropical station (25°N, 137°E) most similar to the environmental conditions at Station ALOHA, they reported a 0-100 m average biomass of $10-30 \mu g C l^{-1}$, which is substantially greater than all previous studies in the NPSG (Table S-2, row #7). They do acknowledge that they used larger (termed "older"; Yamaguchi et al., 2004) conversion factors to allow a comparison with their previously published work. Applying what they describe as the newer conversion factors of 11, 35, and 100 fg cell⁻¹ for heterotrophic bacteria, *Prochlorococcus*, and *Syn*echococcus, respectively, would reduce their biomass-C estimates by at least 50%. At all depths, "heterotrophic bacteria" accounted for 50% of the total plankton biomass, followed by a large, but more variable with depth, contribution of protozooplankton (average ~20% of total).

Sohrin et al. (2010) conducted an extensive study of full ocean depth profiles of prokaryotes, heterotrophic nanoflagellates (HNF), and ciliates along a transect at 160° W in the North Pacific Ocean from the equator to the subarctic region, including three stations in the NPSG. Their total microbial biomass-C estimates for the upper euphotic zone (0–100 m) of the three subtropical stations averaged 27.7 μ g C l⁻¹, with phytoplankton as the dominant component (71%; Table S-2, row #8). Again, this estimate is substantially greater than most others. Their use of a single C:Chl α conversion factor of 157 throughout the entire 0–100 m depth range may have led to an overestimation of phytoplankton C at these stations.

More recently, Pasulka et al. (2013) reported the temporal dynamics of microbial biomass at Station ALOHA over a 6-yr period (2004–2009). This comprehensive study employed a variety of methods including flow cytometry for autotrophic picophytoplankton (Prochlorococcus and Synechococcus) and epifluorescence microscopy of DAPI-stained samples for nano- and microplankton. Eukaryotic cells were binned into eight functional groups based on size, shape, and fluorescence characteristics. The abundant picocyanobacterium Prochlorococcus, which was not included in the Beers et al. (1975, 1982) studies, comprised 30-50% of the total autotrophic biomass in both the upper (0-50 m) and lower (75-125 m) portions of the euphotic zone. Picophytoplankton, autotrophic eukaryotes, and heterotrophic protists over the 0-125 m portion of the euphotic zone ranged from \sim 6–9 µg C l⁻¹, 5–7 µg C l⁻¹, and 5–7 µg C l⁻¹, respectively (Table S-2, rows #9–11), with both seasonal and depth variability. They also reported a seasonal shift in the autotrophic: heterotrophic biomass ratios from >1.3 in winter-spring seasons to <0.7 in summer-fall (Pasulka et al., 2013). The condition of biomass dominance by heterotrophic microorganisms in the euphotic zone, an "inverted trophic pyramid" for the planktonic community, is a common feature of oligotrophic marine ecosystems due to high turnover rates of the autotrophic biomass and high percentages of non-living particulate matter (Gasol et al., 1997). As in the previous studies by Beers (1975, 1982), the autotrophic eukaryote assemblage was dominated by prymnesiophytes and flagellates, with diatoms representing only a few

percent of total biomass-C (Pasulka et al., 2013). The sum of the mean values for these three microbial groups exceeds the mean total microbial biomass of 7.8 μg C l^{-1} derived from the 30-yr mean P-ATP concentrations. This is likely a result of inaccuracies or biases in the assumed P-ATP to biomass-C and per cell C quotas, extrapolations that are used for these independent studies. For example, Pasulka et al. (2013) assumed that *Prochlorococcus* had a constant C quota of 32 fg C cell $^{-1}$, whereas more recent research at Station ALOHA reported a value of $\sim\!26$ fg C cell $^{-1}$ for *Prochlorococcus* in surface waters (Casey et al., 2019).

Finally, Rii et al. (2016) reported the abundance, biomass, and $^{14}\text{C-}$ based primary production attributable to picophytoplankton (<3 µm) at Station ALOHA over a 1-year period. They employed flow cytometrically derived forward scatter to estimate biovolumes, and a C-to-biovolume conversion factor of 237 fg C µm $^{-3}$. Average picophytoplankton biomass in the 0–125 m region of the water column varied considerably (range = 1.2 to 3.0 µg C l $^{-1}$) over the 1-yr observation period (Rii et al., 2016), with *Prochlorococcus* comprising the dominant (61–78%) portion of total picophytoplankton biomass. These estimates by Rii et al. (2016) of *Prochlorococcus* biomass (0.9–2.0 µg C l $^{-1}$; Table S-2, row #12) at Station ALOHA are ~25–30% of the biomass-C values for *Prochlorococcus* reported by Pasulka et al. (2013) for the same location. This underscores the importance of assumptions used to extrapolate cell abundances to biomass, and the challenge in obtaining accurate estimates of total or taxon-specific microbial biomass in the NPSG.

Neither Beers et al. (1975, 1982), Pasulka et al. (2013), nor Rii et al. (2016) evaluated the contribution of heterotrophic bacteria to total microbial biomass-C in the NPSG. Bacterial cell abundances in the upper 0-100 m of the water column at Station ALOHA average 3.8 to 4.8×10^8 cells l^{-1} with peak values generally at 45 m, similar to the P-ATP profile. The C quotas for high-scatter (HS) versus low scatter (LS) cells at Station ALOHA vary considerably and are log normally distributed with mean (median) values of 26.6 (22.6) and 6.7 (5.9) fg C cell⁻¹, respectively (Casey et al., 2019). Consequently, accurate bacterial biomass estimation also requires data on the proportion of the two populations with depth and over time. For the limited data that are available from Station ALOHA, the smaller (LS) cells dominate (>75%) the heterotrophic bacterial assemblage (Casey et al., 2019), resulting in a populationweighted mean (median) of 11.6 (10.0) fg C cell⁻¹. This value is indistinguishable from an estimate previously derived using inverse modeling of Station ALOHA observations (Christian and Karl, 1994) and later used by Björkman et al. (2000) to constrain non-pigmented prokaryotic biomass (i.e., heterotrophic bacteria) in the Climax region, is larger than the 6.3 ± 1.6 fg C cell⁻¹ reported by Kawasaki et al. (2011) for surface dwelling heterotrophic bacteria at Station ALOHA but is similar to the value of 12.8 fg C cell⁻¹ used in the Sohrin et al. (2010) study (Table S-2, row #8). If we assume that the C quota of heterotrophic bacteria is between 5 and 10 fg C cell⁻¹, then the extrapolated biomass-C in the 0-125 m portion of the water column at Station ALOHA would range from 2 to 5 μ g C l⁻¹ (Table S-2, row #13). Combining the Rii et al. (2016) estimates for picophytoplankton with these estimates for heterotrophic bacteria, the total microbial biomass would be $3-7~\mu g$ C l^{-1} compared to 6–8 μg C l^{-1} based on P-ATP (Table S-2, row #14). The higher P-ATP estimate would also include eukaryotes $>3 \mu m$, although the Beers et al. (1975) estimates for microplankton (2–200 μ m) in the Climax region appear to be high relative to the P-ATP based total microbial biomass at Station ALOHA.

In theory, P-ATP concentrations in nature track microbial biovolume more closely than biomass, per se, since intracellular ATP concentrations are buffered at $\sim\!1\text{--}2$ mM to optimize cellular energy transduction reactions (Chapman and Atkinson, 1977). Consequently, we can also estimate total living biovolume from P-ATP for comparison to total particle biovolume measured using optical techniques to obtain an independent constraint on the relative proportion of living to nonliving particles. During a series of cruises to Station ALOHA in Jul-Sep 2012, Barone et al. (2015) measured total particle abundances (1.25–100 μm) and particle size spectra (32 logarithmically spaced size classes) in the

euphotic zone (0-200 m) using a small-angle, forward-scattering laser diffraction instrument (LISST-100X, Sequoia Scientific). Total particle volume was consistently elevated between 20 and 80 m, averaging $0.076 \pm 0.014 \, \mu l \, l^{-1}$, and was dominated by particles in the 3–10 μm size range (Barone et al., 2015). Using the mean P-ATP concentrations at Station ALOHA in the 25–75 m depth range (\sim 32 ng l⁻¹), and assuming 1.5 mM as the average intracellular ATP concentration in living cells (range 1-2 mM ATP; Chapman and Atkinson, 1977), we estimate a biovolume of 0.048 μ l l⁻¹, or ~62% of the total particle volume is comprised of living cells. However, the P-ATP based biovolume estimate would also include living particles that are below the 1.25 μm detection limit of the LISST-100X (e.g., picocyanobacteria and heterotrophic bacteria) so the \sim 62% value is an upper constraint. This comparison of two independent estimates of total particle volume to biovolume from P-ATP supports the conclusion that nonliving particles comprise a large portion of the PC pool and, hence, particle volume at Station ALOHA.

White et al. (2017) also used in situ optical techniques to distinguish living from nonliving C at Station ALOHA. Based on high frequency (1 min underway sampling resolution) measurements of the beam attenuation coefficient (Cp) at 660 nm, an optical proximity for PC in the 0.2-2.0 µm size range (Siegel et al., 1989), they were able to resolve a diel-oscillating pattern in C_p which was attributed to the dynamics of living C superimposed on a non-replicating, nonliving, detrital PC background value. The Cp proxy at Station ALOHA demonstrated that the diel amplitude, with maximum values near sunset and minima at sunrise, reflected a balance between net particle accumulation due to photosynthesis and net nighttime loss due to respiration and other processes (White et al., 2017; Henderikx-Freitas et al., 2021). By comparing this high frequency diel C_p pattern with P-ATP collected on 37 HOT cruises at near monthly intervals for a 6-yr period (2015–2020), and assuming two different C:ATP ratios of 250:1 and 400:1 (based on the analysis of Christian and Karl, 1994), the mean living portion of total PC ranged from 27 \pm 8% (for C:ATP = 250:1) to 42 \pm 12% (for C:ATP = 400:1), once again supporting the conclusion of dominance of particulate detritus in the upper portion of the euphotic zone at Station ALOHA (Henderikx-Freitas et al., 2021). While large changes (2-3 fold) were observed for both the baseline (detrital C) and the diel amplitude (living C) from cruise to cruise, there was no clear seasonality in either PC fraction for near-surface ocean samples. Day-to-day variability of C_p amplitude within cruises (average 17%) was nearly as large as month-tomonth variations (average 21%), indicating significant spatial or high frequency temporal variability in both productivity and in the proportion of living C (Henderikx-Freitas et al., 2021). Similar high frequency variability in oxygen-derived gross primary productivity, respiration, and net community production has previously been reported in the NPSG (Nicholson et al., 2015; Barone et al., 2019).

Given the difficulties in enumerating the broad size spectrum and phylogenetically diverse microbial assemblage at Station ALOHA, and the even greater challenge of estimating total living organism biovolume, it should come as no surprise that the microbial biomass-C estimates obtained using different methods do not always converge. The P-ATP derived microbial biomass-C values are generally lower than those obtained using microscopic and flow cytometric estimates (see Table S-2), and inclusion of bacterial biomass to the enumeration methods would only lead to even larger discrepancies. Furthermore, whereas the microscopic assessments show considerable decreases with depth within the upper euphotic zone (0–100 m) and large seasonal variability, the microbial biomass estimates based on P-ATP concentrations are relatively constant with depth (0–100 m) with only small seasonal changes (Fig. 1a inset, Fig. 2, and Table S-1).

An intriguing result of our 30-yr P-ATP time series is the perennial peak that we observe at 45 m, a feature not seen in microbial biomass estimation by microscopic and flow cytometric methods, which instead generally report maxima for the upper euphotic zone (0–25 m; Beers et al., 1975; Pasulka et al., 2013; Rii et al., 2016). The "peak" in P-ATP could be interpreted as either increased concentrations at 45 m or

depressed P-ATP concentrations in the upper 0-25 m portion of the euphotic zone, relative to total microbial biomass (i.e., a lower intracellular ATP concentration and higher C:ATP ratio for microorganisms in near-surface waters). It is well known that phosphate limitation decreases cellular ATP (and increases the C:ATP ratio) in a variety of microorganisms (Sakshaug and Holm-Hansen, 1977; Karl, 1980), and the surface waters at Station ALOHA are chronically depleted in phosphate (Karl and Tien, 1997). Karl et al. (1995) reported a significant decrease in surface P-ATP and corresponding increase in the C:ATP ratio at Station ALOHA in response to the 1991-1992 El Niño event, despite increases in primary production and photosynthetic assimilation number (mg C mg Chl a^{-1} h⁻¹). Letelier et al. (1996) later developed a more generalized model regarding phosphate depletion and decreased intracellular ATP concentrations in surface waters at Station ALOHA that occurred despite active microbial growth. We examined the relationships between surface (5 and 25 m) phosphate concentrations and P-ATP concentrations to determine whether there was any evidence to support the hypothesis that phosphate stress may alter the in situ C:ATP ratio of microbes at Station ALOHA. Assuming a relatively constant microbial biomass in the surface waters, the phosphate stress effect would be manifested as a decrease in P-ATP at phosphate concentrations below the reported threshold of 50–60 nmol kg⁻¹ for phosphate limitation at Station ALOHA (Letelier et al., 2019). The results of this analysis failed to document any trend and, if anything, the P-ATP values are higher, not lower, at phosphate concentrations < 50 nmol kg⁻¹ (Fig. S-1). Consequently, there is no evidence to support a change in the biomass-C to P-ATP relationship in the upper euphotic zone at Station ALOHA. Alternatively, the microscopic methods might overestimate biomass-C in the near surface waters due to the inability to distinguish between live and dead cells, or to a systematic depth-dependent change in the abundanceto-biovolume-to-biomass extrapolation.

Finally, Kawasaki et al. (2011) used a novel biomarker approach to estimate the biomass-C of heterotrophic bacteria as well as the contribution of bacterial detrital C to the total PC pool at Station ALOHA from surface waters to the bathypelagic zone. By measuring muramic acid (MA), D-Alanine (D-Ala), and D-Glutamic (D-Glu) acid (unique biomarkers for bacteria; see McCarthy et al., 1998), they were able to constrain total bacterial biomass and estimate the amount of nonliving C that had been derived from previously living heterotrophic bacteria, information that cannot be obtained by any other means. The concentrations of all three bacterial biomarkers were greatest in the upper 0-100 m, decreasing rapidly throughout the lower euphotic zone upper mesopelagic zone transition, then remaining relatively constant in the bathypelagic zone (2000-4000 m; Kawasaki et al., 2011). These depth patterns are nearly identical to those observed for P-ATP reported herein. Kawasaki et al. (2011) also estimated that the C content of surface dwelling heterotrophic bacteria at Station ALOHA accounted for 6.8 \pm 1.1% of the total PC pool. Living cyanobacteria in their study accounted for 13.3 \pm 2.2%, so the total prokaryotic biomass in the 0–100 region of the water column was 5 μ g C l⁻¹, or ~20% of the total PC (Kawasaki et al., 2011). Based on these extensive studies and on our own P-ATP 30-yr time series, total microbial biomass in the upper euphotic zone at Station ALOHA is likely constrained to a value between 5 and 10 μ g C l⁻¹ throughout the year.

4.2. Stochastic variability in microbial biomass inventories: upper euphotic zone

Pasulka et al. (2013) evaluated the role of episodic deep winter mixing as a possible control on autotrophic eukaryotic abundance and biomass at Station ALOHA for the period Jun 2004 – Jan 2009. It had previously been shown that deep winter mixing events can occasionally penetrate to the top of the nutricline and deliver nitrate and phosphate to the euphotic zone (Karl et al., 2001), possibly leading to a phytoplankton bloom. The deepest mixed layer in the Pasulka et al. (2013) time-series (~140 m using the 0.125 potential density criterion) was

observed in Jan 2006, but neither the abundance nor the biomass of autotrophic eukaryotes "was notably elevated" compared to the winter values observed in Feb 2005, Dec 2007, and Dec 2008. However, they also noted that nitrate concentrations were not elevated in the upper 0–100 m during the Jan 2006 expedition despite the relatively deep mixed layer. Since the coupling mechanisms and dynamics of nutrient delivery, uptake, and subsequent export are not well constrained, it is likely that nutrients delivered to the upper euphotic zone were rapidly drawn down to background concentrations. Consequently, they were unable to determine whether bottom-up processes including aperiodic, advective nutrient fluxes were important controls on microbial biomass in the near-surface waters at Station ALOHA.

We re-evaluated the relationships between deep mixing, nitrate delivery to the euphotic zone, and total microbial biomass-C using the much longer 30-year time series at Station ALOHA. For this analysis, we used two different mixed layer depth criteria, namely the 0.125 potential density difference from the surface and the 0.03 potential density difference from 10 m, with the latter always returning a shallower mixed layer depth at Station ALOHA (see Karl et al., 2021). Since each CTD hydrocast for a given expedition has a unique mixed layer depth estimate, we report the mixed layer depths for both the P-ATP hydrocast as well as the standard deviations for each ~3-day expedition, compared to the 30-year climatologies for each month (Table 5). Only those cruises where mixed layer depth for the P-ATP hydrocast exceeded 125 m (0.125 density criterion) and 100 m (0.03 density criterion) are considered to be physical perturbations relative to the 30-year monthly climatology (Table 5). With one exception (cruise 104, Apr 1999), all remaining deep mixing events were in winter (Dec-Feb) when the upper water column is least stratified and surface cooling is at its annual maximum. The 0-100 m depth-integrated P-ATP concentrations coinciding with these physical perturbations ranged from 1.9 to 2.9 mg m $^{-2}$, and were not systematically elevated compared to the corresponding 30year monthly climatologies. We independently evaluated the relationships among 0-100 m depth-integrated nitrate inventories (presumably a consequence of past or present deep mixing; Karl et al., 2001) and P-ATP. We used a threshold of 6 mmol nitrate m⁻² and, by this criterion, our analysis of the 30-year time series identified 10 high nitrate perturbations (Table 6). The nitrate inventories ranged from 6.1 to 19.6 mmol m⁻² and, as expected, most of the cruises with elevated 0–100 m nitrate were in late fall and winter seasons (Nov-Feb; Table 6). An unexpected result was that none of the 10 elevated surface nitrate cruises coincided with any of the 9 cruises with deepest mixed layers (see Table 5), as one might expect if deep mixing penetrated the top of the nutricline and redistributed nitrate throughout the upper euphotic zone. One likely explanation for this, as well as the relatively large range of observed concentrations in the upper 0-100 m portion of the water column, is the enormous capacity for rapid nutrient uptake and assimilation by the nutrient-depleted microbial communities in the NPSG (McAndrew et al., 2007). Consistent with the deep mixed layer analyses (Table 5), the 0–100 m P-ATP inventories observed during the elevated nitrate cruises were not systematically higher than the respective monthly P-ATP climatologies (Table 6). Based on these ten cruises where the 0-100 m nitrate inventory was unusually high, the mean difference in the 0-100 m P-ATP inventory from the long-term monthly climatology ranged from -0.9 to +0.8 mg m⁻², with a mean value of +0.02mg m $^{-2}$ per event, a value that is equivalent to \sim 0.3% of the inventory (Table 6).

Rii et al. (2021) recently evaluated the resilience of the picoeukaryotic community diversity and structure to episodic-scale physical disturbances, including mixing, using data collected at Station ALOHA. They concluded that while mixing can redistribute microorganisms relative to pre-disturbance gradients in light and nutrients, community structure was relatively resilient and recovered from physical perturbation on the order of days to weeks, a time scale that is less than the average interexpedition period (~40 d) for our time-series sampling at Station ALOHA. Consequently, the absence of a predicted increase in

Table 5 Impacts of deep mixed layers on 0–100 m depth-integrated P-ATP inventories.

	Mixed Layer Depth (
Cruise # and Date	0.125 Density Criteri	0.125 Density Criterion		0.3 Density Criterion		
	ATP cast cruise mean (cruise SD, n)	Monthly climatology mean (SD, n)	ATP cast cruise mean (cruise SD, n)	Monthly climatology mean (SD, n)	P-ATP inventory (mg m ⁻²)	Monthly climatology (mg m ⁻²)
3	133	91	126	69	2.8	2.8
Jan 1989	118 (10, 15)	(27, 23)	114 (10, 15)	(26, 23)	(0.1)	(0.7)
101	142	91	106	69	2.7	2.8
Jan 1999	127	(27, 23)	73	(26, 23)	(0.1)	(0.7)
	(15, 15)		(40, 15)			
104	129	57	115	39	2.8	3.3
Apr 1999	128 (13, 13)	(27, 23)	82 (41, 13)	(19, 23)	(0.1)	(0.5)
144	121	91	118	69	2.7	2.8
Jan 2003	79	(27, 23)	113	(26, 23)	(0.1)	(0.7)
Jan 2003	(15, 15)	(27, 23)	(8, 14)	(20, 20)	(0.1)	(0.7)
208	129	91	100	69	2.6	2.8
Jan 2009	110	(27, 23)	83	(26, 23)	(0.1)	(0.7)
	(14, 15)		(15, 15)			
238	132	85	114	68	2.7	2.7
Dec 2011	118	(22, 25)	100	(25, 25)	(0.1)	(0.5)
	(11, 15)		(12, 15)			
249	124	72	104	50	1.9	2.7
Feb 2013	111	(27, 26)	77	(23, 26)	(0.1)	(0.7)
	(37, 15)		(37, 15)			
268	123	85	121	68	2.3	2.7
Dec 2014	107	(22, 25)	105	(25, 25)	(0.1)	(0.5)
	(10, 14)		(10, 14)			
290	121	72	114	50	2.9	2.7
Feb 2017	114	(27, 26)	101	(23, 26)	(0.1)	(0.7)
	(11, 15)		(14, 15)			

total microbial biomass-C, with either deep mixing or nitrate intrusion into the upper euphotic zone, is consistent with the plankton community resilience hypothesis presented by Rii et al. (2022). The relative uniformity of the 0–100 m depth-integrated P-ATP inventory, despite seasonal and stochastic variations in environmental variables over the 30-year observation period, is an excellent example of ecosystem homeostasis. The predictability of P-ATP in the 0–100 m region of the water column and the lack of any systematic response in total microbial biomass-C to deep mixing and allochthonous nutrient delivery was unexpected. Out of 277 cruises, there were only five (cruises 51/Jan 1994, 53/Mar 1994, 57/Sep 1994, 117/Jul 2000, 214/Aug 2009) where the

0–100 m depth-integrated P-ATP inventories exceeded 2 standard deviations of the long-term mean value of 3.1 (SD = 0.7, n = 277) mg m $^{-2}$. There was nothing particularly unusual about any of these cruises (e.g., PC inventories, inorganic nutrient concentrations, primary production, or particulate C export) that might have led to a higher than expected microbial biomass, so these anomalies are currently unexplained. It should be mentioned that 3 of the 5 cruises were in 1994, one of two years where 0–100 m depth-integrated P-ATP was consistently elevated relative to the 30-year mean (Fig. 4).

Finally, Liu and Levine (2021) presented a novel model to explore the ecological impacts of short-lived upwelling events at Station ALOHA.

 $\begin{tabular}{ll} \textbf{Table 6} \\ \textbf{Impacts of elevated nitrate plus nitrite (N+N) inventories on 0-100 m depth-integrated P-ATP.} \\ \end{tabular}$

Cruise # and Date	$_{\rm N+N}$ inventory (mmol m $^{-3}$)	N+N monthly climatology $(\mu mol\ m^{-3})$	Cruise P-ATP inventory (mg m ⁻²)	P-ATP monthly climatology (mg m ⁻²)	P-ATP difference cruise-climatology mg m ⁻² (%)
14	9.1	2.2	2.6	2.7	-0.1
Feb 1989		(3.8)	(0.1)	(0.7)	(-3.7)
45	10.8	2.2	3.3	2.7	+0.6
Feb 1993		(3.8)	(0.1)	(0.7)	(+22)
82	19.6	1.8	4.1	3.3	+0.8
Apr 1997		(6.5)	(0.2)	(0.5)	(+24)
109	6.1	1.8	3.3	3.1	+0.2
Nov 1999		(3.6)	(0.1)	(0.7)	(+6.5)
133	18.4	1.9	2.9	2.7	+0.2
Dec 2001		(3.9)	(0.1)	(0.5)	(+7.4)
135	14.8	2.2	2.0	2.7	-0.7
Feb 2002		(3.8)	(0.1)	(0.7)	(-26)
141	6.7	1.8	2.2	3.1	-0.9
Nov 2002		(3.6)	(0.1)	(0.7)	(-29)
168	16.3	1.1	3.4	3.1	+0.3
Mar 2005		(2.4)	(0.1)	(0.9)	(+10)
289	9.8	1.9	2.4	2.7	-0.3
Dec 2017		(3.9)	(0.1)	(0.5)	(-11)
305	10.9	0.6	3.4	3.3	+0.1
Sep 2018		(0.7)	(0.1)	(0.8)	(+3.0)

They focused their ecosystem simulations on the late winter - early spring (Feb-Apr) period, when "excess" nitrate is often detected, and explored a range of disturbance intensities and durations, the latter from 1 to 7 days. The greatest competitive advantage for large phytoplankton (i.e., diatoms) was during high intensity (\sim 40 m d⁻¹), short-lived (1 day) physical disturbances. Under these conditions, the biomass of their large phytoplankton class increased nearly 30% relative to predisturbance conditions. For disturbances that lasted 1 day, all ecological and biogeochemical impacts were restored to background conditions after 28 days in their model domain. Furthermore, the relationships between mixed layer depth, euphotic zone nitrate inventory, and total microbial biomass (as assessed herein as P-ATP) are complex, and likely temporally decoupled, as we present herein (Tables 5 and 6). Consequently, these model-predicted biomass increases could go undetected in our 0-100 m depth-integrated P-ATP inventory analysis unless the cruise coincided in time with the idealized dynamics presented in their model (Liu and Levine, 2021).

4.3. Microbial biomass and organism attributions: lower euphotic-to-mesopelagic zone transition, and below

Mean P-ATP inventories in the transition region between the lower euphotic and upper mesopelagic zones (100-250 m) were greater than one-half of those in the most productive, 0-100 m region of the water column (Table 2). This relatively high microbial biomass was unexpected because rates of primary production below 100 m are ~10% of the near-surface upper euphotic zone (Karl et al., 2021). Furthermore, the photosynthetic compensation depth at Station ALOHA, where net primary production is zero over a 24-hr period, is ~175 m (Laws et al., 2014), so ecosystems beneath this depth rely entirely on allochthonous sources of organic matter and energy. Within this transition region there are steep gradients in P-ATP and PC; yet there still appears to be a relatively large, viable microbial assemblage throughout the transition zone that is presumably dominated by chemoorganoheterotrophic microorganisms. Indeed, the total depth-integrated microbial biomass below 100 m exceeds that in the upper 0-100 m productive euphotic zone (Table 2), but a quantitative understanding of sources of energy required to sustain these biomass distributions is lacking at the present time (see Biomass distributions: energy and ecology section).

In their original report of microbial biomass beneath the euphotic zone off Southern California (33°19'N, 118°40'W), Holm-Hansen and Booth (1966) documented a rapid decrease in P-ATP in the lower portion of the euphotic zone similar to the trends that we observe at Station ALOHA. However, beneath this zone of rapid P-ATP decrease, Holm-Hansen and Booth (1966) reported a peak in P-ATP at ~400 m reaching concentrations of 34-66 ng l⁻¹ (compared to surface concentrations of ~300 ng P-ATP l⁻¹), before a more gradual decrease at greater depths to much lower P-ATP concentrations (\sim 0.5 ng l⁻¹) at 1025 m. The upper mesopelagic zone peak in P-ATP off southern California also displayed an increase in the ratio of living to total PC (27%), compared to lower values (biomass-C was < 6% of total PC) throughout the remainder of the mesopelagic zone. Several independent studies have also reported subsurface peaks in P-ATP in the upper mesopelagic zone, including profiles collected off California (31°45'N, 120°30'W; Hamilton et al., 1968, and 36°48′N, 121°46′W; Karl and Winn, 1984), off the coast of Peru (09°45'S, 83°37'W; Hamilton et al., 1968), on the mid-Atlantic Ridge and abyssal plain of the North Atlantic Ocean (26°18'N, 44°44'W and 26°51'N, 60°14'W, respectively; Karl et al., 1976), in the Columbia Basin of the Caribbean Sea (10°6.5′N, 77°17′W; Karl, 1979), in the tropical North Pacific Ocean (18°44'N, 156°50'W; Winn and Karl, 1984), and at Station Gollum in the NPSG (22°10'N, 158°W; Holm-Hansen and Paerl, 1972). The broad geographical distribution of this upper mesopelagic zone phenomenon suggests that there might be a common mechanism to produce and sustain these features. Subsurface peaks in P-ATP and PC have also been shown to be local maxima in microbial activity at the core of the O2 minimum, including

in situ rates of RNA synthesis and ATP-specific rates of RNA synthesis (Fellows et al., 1981). Therefore, these mesopelagic regions may be metabolic hotspots supporting subeuphotic zone organic matter remineralization as well as new biomass production. Karl et al. (1976) hypothesized that sinking particulate organic matter, derived from the productive surface ocean, might accumulate on specific isopycnal surfaces as the seawater density at depth approaches that of average organic matter (~1.027 g cm⁻³; Riley, 1970). This allochthonous organic matter could provide the C and energy resources necessary for the net growth and accumulation of microbial biomass. Alternatively, microorganisms associated with the sinking particles could be passively transported downward and contribute to the mesopelagic zone peak in P-ATP, or be actively transported by vertically migrating mesozooplankton (Hamilton et al., 1968). Holm-Hansen (1969) reported peaks in PC and PN at 400 m off the California coast at 30°40′N. 120°02′W, but at that location at that time, there was no detectable P-ATP peak. It is likely that the residence times of PC and P-ATP are variable, as is the flux of PC from the euphotic zone, so these mesopelagic zone phenomena may be ephemeral. While we observe a small (~20%) increase in the 30-yr mean P-ATP at 500 m, there is no detectable increase in PC at the same depth at Station ALOHA (Fig. 1 and Tables 1 and 3). Since the seawater density structure varies geographically, each site is unique, so one would need to conduct specific isopycnal sampling near the 1.027 g cm⁻³ density horizon to test this hypothesis. At Station ALOHA this target density is centered at \sim 675 m, so our standard sampling depths of 500 and 750 m may have missed the 1.027 g cm⁻³ isopycnal P-ATP and PC peaks, if they existed at all.

There are few quantitative microscopic studies that extend into the mesopelagic zone of open ocean ecosystems. Fournier (1966) confirmed previous observations, dating back to reports from the 1925-1927 Meteor expedition, of pigmented microorganisms in the aphotic regions of diverse, pelagic habitats. Because these cells assimilated ¹⁴C-labeled organic substrates (Fournier, 1966), they were judged to be viable and metabolically active. In a comprehensive study of the North Atlantic Ocean using sterile Niskin® bag samplers, a variety of fixation methods, and light and electron microscopy techniques, Fournier (1970) described three separate groups of cells: (1) abundant, small 1-5 µm (but occasionally as large as 15 µm) spherical or ellipsoidal pigmented cells that appeared yellow to brown in color under light microscopy, and possibly prokaryotic because there were no discernible organelles, (2) small 1.3-2.5 µm cells with eukaryotic organelles including chloroplasts, and (3) less abundant, small 1.2 µm cells with little internal differentiation that were often clumped and appeared to be reproducing. The most abundant group, which peaked at a depth of 375-450 m in all 10 North Atlantic stations at $\sim 125 \times 10^3$ cells l⁻¹ (Fournier, 1970), appeared to be identical to the "olive green cells" (OGCs) reported from the Meteor expedition (Hentschel, 1936). Confirmation of Fournier's report came quickly with the analysis of samples collected off the coast of California (31°45'N, 120°30'W; Hamilton et al., 1968). This latter study was able to culture small green autotrophic cells of the same size and appearance as the previously described OGCs from depths to 2000 m, confirming the presence of viable cells. The Hamilton et al. (1968) study also included measurements of P-ATP, so an estimate could be made of the contribution of these enigmatic pigmented cells to aphotic zone microbial biomass. For the 300-1000 m depth region of the water column, the small 1.5–4.5 μ m pigmented cells accounted for only ~5% of the total microbial biomass estimated from P-ATP at this coastal station (Hamilton et al., 1968). Fournier and Holm-Hansen made independent measurements of OGCs and P-ATP at Station Gollum, and reported that OGCs at this oligotrophic site represented a significant percentage of the total microbial biomass, up to 100%, in the mesopelagic and bathypelagic zones (Fournier, 1971; Holm-Hansen and Paerl, 1972). Furthermore, Fournier (1973) documented the presence of OGCs in the digestive tracts of pelagic tunicates collected from 450 to 750 m in the NPSG, thereby providing direct evidence of a mesopelagic sink for OGCs. Gowing and Silver (1985) have also reported the presence of small fecal pellets ("minipellets," $3-50~\mu m$ in diameter) collected in sediment traps at various depths (80–2000 m) in the eastern tropical North Pacific Ocean, some of which were identical in appearance to OGCs. The process required to sustain this sub-euphotic zone population distribution of OGCs remains poorly understood. But, it may be related to particulate matter export from the euphotic zone, as suggested by Gowing and Silver (1985), even though the OGCs were rare in both surface waters and in the digestive tracts of tunicates collected in the euphotic zone (Fournier, 1973). Alternatively, Sorokin et al. (1985) hypothesized that OGCs may be cysts of small ($3-6~\mu m$) microflagellates.

It is expected that heterotrophic microorganisms, especially freeliving and particle-associated bacteria, would dominate the total microbial biomass throughout the meso- and bathypelagic regions of the water column. Accurate quantitative determinations of bacteria became possible only after the introduction of fluorescent dyes and epifluorescence microscopy, combined with the use of polycarbonate membrane filters (e.g., Hobbie et al., 1977). However, the small size of marine bacteria, changes in cell size upon fixation, the "halo-effect" of fluorescent dyes, and the inability to distinguish between live and dead cells precluded accurate biovolume and, therefore, biomass determinations (Daley, 1979). As a complementary approach, Watson et al. (1977) devised a novel method to estimate the biomass of gram-negative bacteria based on the measurement of particulate lipopolysaccharide (P-LPS). Laboratory-based estimates of the C:LPS ratio of a variety of morphologically and taxonomically diverse bacteria converged on a value of 6.35:1, and this was adopted for use in the field to estimate bacterial biomass throughout the water column in a variety of open ocean habitats. In one study, Watson and Hobbie (1979) compared mesopelagic zone microbial biomass derived from P-ATP, epifluorescence microscopy, and P-LPS using conversion factors of 250:1 (C: ATP), 10 fg C bacterial cell⁻¹, and 6.35:1 (C:LPS) for 11 samples collected throughout the mesopelagic zone (200-1800 m) at a station off the southwest coast of Africa. The LPS-derived estimate of bacterial biomass was on average 135% (range 82-275%, median 117%) of the direct count estimate of bacterial biomass, and was 85% (range 53-146%, median 90%) of the total microbial biomass derived from P-ATP (Watson and Hobbie, 1979). These results suggest that gramnegative bacteria are the dominant biomass component throughout the mesopelagic zone in this region of the world's ocean.

Shibata et al. (2006) measured particulate peptidoglycan (P-PG), a unique biomarker for bacteria, at several stations in the western Pacific Ocean off Japan. P-PG concentrations were well correlated with bacterial abundance measured using epifluorescence microscopy. However, based on measured P-PG per bacterium, they concluded that most of P-PG (≥85%), especially in the bathypelagic zone, must be associated with particulate detritus of bacterial origin, rather than with living cells. These results confirmed previous observations of Benner and Kaiser (2003) and Kawasaki et al. (2011) using an independent set of bacterial biomarkers (see Particulate matter: sampling, size distribution, composition, and stoichiometry section).

One of the most comprehensive reports of mesopelagic and bathypelagic bacterial biomass in the North Pacific Ocean included several stations in subtropical ecosystems to depths of ~6000 m (Nagata et al., 2000). Bacterial biomass was extrapolated from cell abundances using epifluorescence microscopy, assuming 15 fg C cell⁻¹, a value that was 50% higher than the conversion factor used in the Watson and Hobbie (1979) field study. Several interesting features included: (1) a depthintegrated bacterial biomass in the 1000-4000 m region of 0.7-1.4 g C m⁻², a value that was equivalent to that observed for total phytoplankton biomass in the euphotic zone $(0.5-1.2 \text{ g C m}^{-2})$, and consistent with the P-ATP derived microbial biomass versus depth distributions from Station ALOHA (Table 2), (2) a vertical profile of bacterial abundance and metabolic activity (as determined by ³H-leucine incorporation) that statistically fit a log-log transformed power function similar to that described by Martin et al. (1987) for the downward flux of particulate organic matter (see Biomass distributions: energy and ecology

section), and (3) an estimated turnover time of 2.6-18 yr for bacterial biomass in the 1000-4000 m depth region. The authors acknowledged that the rates of ³H-leucine incorporation may have been underestimated by up to a factor of six since they were not conducted under in situ conditions of hydrostatic pressure, so the actual turnover times are probably much faster. Furthermore, they also acknowledged that the total bacterial cell abundances they report may include inactive, dormant, and "ghost" (i.e., dead; Zweifel and Hagström, 1995) cells, so both bacterial biomasses and turnover times may be in error. Nevertheless, this comprehensive study stands as a benchmark for our understanding of bathypelagic microbial ecology. Based on the assumption that the bacteria enumerated in their study were chemoorganoheterotrophic, they concluded that the source of carbon and energy required to support the bathypelagic food web must be the rain of detrital materials ultimately produced in the euphotic zone, and thus supported the Cho and Azam (1988) model that sinking particles are solubilized to release dissolved organics that support the free-living heterotrophic bacteria throughout the water column (see Biomass distributions: energy and ecology section).

Several recent studies of microbial biomass in subeuphotic zone habitats report "prokaryotes" as the dominant group (Sohrin et al., 2010; Pernice et al., 2015). This term includes both heterotrophic bacteria plus Archaea, without further distinction between these fundamentally distinct microbes. It was initially thought that Archaea were relegated to Earth's most extreme environments until they were later discovered to be abundant and ubiquitous components of marine plankton in both coastal and open ocean habitats (DeLong, 1992; Fuhrman et al., 1992). Because extant epifluorescence-based microscopic methods used for "bacterial" cell enumeration (e.g., Nagata et al., 2000) cannot distinguish between the domains Bacteria and Archaea, previous estimates of bacterial biomass by direct epifluorescence microscopy could be called into question. Karner et al. (2001) employed rRNA-targeted fluorescent probes to independently enumerate Bacteria and Archaea at Station ALOHA over a 1-yr period (1997-1998). The two archaeal and one bacterial probes targeted viable cells and together detected >80% of the total DAPI-stained cells, which set an upper limit of ~20% of total cell abundance for the contribution of ghost cells in the mesopelagic and bathypelagic zones at Station ALOHA. Their results documented a domain shift below ~100 m with Crenarchaeota (Marine Group I Archaea) increasing in relative proportion to achieve equity with Bacteria below ~1000 m (Karner et al., 2001). No biovolume estimates were provided in this study, but a previous investigation of several deep water stations in the eastern North Atlantic Ocean (Patching and Eardly, 1997) reported that "bacterial" cell biovolumes were relatively constant over the entire water column with mean values ranging from 0.03 to 0.05 μm³ and a biovolume-frequency distribution that was skewed towards smaller cells. As long as there is no size (biovolume) bias between planktonic Bacteria and Archaea, the previous misattribution of Archaea is of no consequence in estimating "bacterial" biomass from cell abundances. However, the metabolic capabilities, growth rates, and biogeochemical functions of these two distinct groups may be fundamentally different, so combining them into the category prokaryotes may complicate the ecological interpretations of energy flow. For example, Herndl et al. (2005) reported that some Archaea are chemolithoautotrophic, using reduced inorganic substrates (e.g., ammonium) as energy sources and carbon dioxide as a C source. In support of the existence of Crenarchaeal chemolithoautotrophy, Church et al. (2010) presented observations from a range of North Pacific mesopelagic habitats, including Station ALOHA, documenting the ubiquity of Crenarchael amoA genes and transcripts throughout the mesopelagic zone, suggesting a metabolic potential for chemolithotrophic ammonium oxidation. However, the authors were quick to point out that their results do not preclude chemolithoorganotrophy, the simultaneous oxidation of ammonium and assimilation of organic substrates as previously shown for Crenarchaeota in other marine habitats. However, if the metabolic balance was favor

chemolithoautotrophy, then a source of reduced inorganic substrates would need to be identified for net carbon fixation to occur well beneath the euphotic zone (see **Biomass distributions: energy and ecology** section). Studies using whole genome sequence analysis of sorted, uncultured *Proteobacteria* cells sampled from the mesopelagic zone of Station ALOHA reported genomic evidence for sulfur-based chemolithoautotrophy (Swan et al., 2011), and it has also been suggested that nitrite-oxidizing bacteria may play a major role in deep ocean inorganic carbon fixation (Pachiadaki et al., 2017). The balance between mesoand bathypelagic zone autotrophy versus heterotrophy needs to be reconciled, given its importance for modeling C and energy flows in pelagic ecosystems (Herndl and Reinthaler, 2013).

There are relatively few quantitative reports of eukaryotic microorganisms in the meso- and bathypelagic zones of the ocean. Morgan-Smith et al. (2011) provide one of the most comprehensive assessments for a series of stations in the subtropical and tropical North Atlantic Ocean. By combining a catalyzed reporter deposition-fluorescence in situ hybridization (CARD-FISH) method using two independent eukaryotic probes (EUK516 and KIN516) with more conventional epifluorescence microscopy, they were able to enumerate, size, and differentiate (based on morphology) 9 categories of eukaryotic microorganisms to depths of 5000 m. The general pattern displayed an exponential decrease in total abundance from 100 to 900 m, followed by near constancy of eukaryotic cell numbers from 1000 to 5000 m. The cell numbers at depths >1500 m ranged from 6.4 to 32 cells ml⁻¹ (for epifluorescence microscopy) compared to 0.68-6.4 cells ml⁻¹ for the CARD-FISH method (Morgan-Smith et al., 2011). Kinetoplastids (detected using the universal KIN516 probe) were abundant, ranging from 16 to 27% of the total eukaryotic cells (detected using the universal EUK516 probe). This study also evaluated the effects of hydrostatic pressure by comparing paired samples from 2750 and 4000 m that were collected using pressure-retaining titanium chambers that allowed fixation either before or following depressurization. No difference was found in the number of eukaryotes detected. A follow-on study in the tropical and subtropical North Atlantic, using similar analytical methods, collected samples to a depth of 7000 m. This latter study used six different CARD-FISH probes to enumerate a variety of taxonomically distinct groups of eukaryotes. As in the previous study, cell abundances using CARD-FISH were lower, by up to an order of magnitude, compared to the fluorescent microscopic technique (Morgan-Smith et al., 2013). Unfortunately, no total eukaryote biomass estimates were presented in either study.

Finally, Pernice et al. (2015) investigated the abundances and biomasses of prokaryotes and heterotrophic protists in the "dark ocean" at 116 stations worldwide as one component of the Malaspina 2010 expedition, including multiple stations in the NPSG. Three complementary techniques (epifluorescence microscopy, fluorescence in situ hybridization using a eukaryote probe, and flow cytometry) were used. Cell biovolumes were extrapolated to biomass-C using previously published relationships (Menden-Deuer and Lessard (2000) for protists and Gundersen et al. (2002) for prokaryotes). Global average heterotrophic protist biomass decreased from \sim 280 ng C l^{-1} in the upper mesopelagic zone to 50 ng C l^{-1} in the bathypelagic zone. Prokaryote biomass-C was 2.6 times greater than heterotrophic protists in the mesopelagic zone and 4.8 times greater in the bathypelagic zone, documenting a systematic increase in the prokaryote-to-protist biomass-C with depth. In a follow-on study, Pernice et al. (2016) reported the taxonomic diversity of bathypelagic zone microbial eukaryotes (0.8-20 µm) for the global ocean, including several stations in the NPSG. They employed pyrosequencing of the V4 region of the 18S rRNA gene to examine the taxonomic diversity of deep-sea microbial communities. Each 100-l deep seawater sample contained between 400 and 1000 "operational taxonomic units" (OTUs, binned as pyrotags with a 97% sequence similarity threshold); the pooled samples revealed a global richness of ~2500 OTUs (Pernice et al., 2016). At the taxonomic level, Rhizaria (53%) and Alveolata (18%) were the most abundant supergroups.

4.4. Particulate matter: sampling, size distribution, composition, and elemental stoichiometry

Quantitative sampling of suspended particulate matter might appear to be simple and straightforward, but this is not the case. First, one must select between a range of screens (constructed from metal or plastic) or membranes (composed of cellulose esters or glass fibers) each with unique retention characteristics. Head-to-head comparisons have shown that the metal filters retain particles that are similar to the nominal pore size whereas the glass fiber filters used in our study retain particles much smaller than the nominal pore size, even for small sample sizes and low particle concentrations (Sheldon, 1972). For example, Viviani et al. (2015) found no significant differences in Chl a concentrations for GF/F and 0.2 µm porosity Nuclepore® filters at Station ALOHA. The dominant Chl a-containing microorganism at Station ALOHA, Prochlorococcus, has a size distribution that is smaller than the 0.7 µm nominal porosity of the GF/F filters (80 \pm 3% of cells are in 0.35–0.65 μm interval; Casey et al., 2019), documenting the much smaller effective porosity, as previously shown by Sheldon (1972).

The present study used glass fiber filters to operationally define the boundary between dissolved and particulate matter. However, the size spectra for P-ATP and PC are likely to be quite different. While the glass fiber filters used in this study probably capture the majority of P-ATP in the ocean (note: P-ATP concentrations using Whatman GF/F filters generally equal or exceed P-ATP concentrations using 0.2 µm polycarbonate membranes), this is not true for nonliving particles. Indeed, Altabet (1990) reported that 0.2 µm aluminum oxide Anopore® filters collected ~40% more PC and ~31% more PN than the more commonly employed Whatman GF/F filters for samples collected in different seasons at a station in the oligotrophic Sargasso Sea. However, the particles retained on Anopore filters but not retained on GF/F filters, had nearly identical PC:PN ratios (Anopore PC:PN molar ratios were only 5% (SD = 5%) higher than GF/F filters; Altabet, 1990). We justify our use of GF/F filters for PC and PN analyses because they are matched with our P-ATP determinations, and because it is probable that the GF/F filters efficiently collect most, if not all, living microorganisms.

In a series of high-profile papers, R. Benner's laboratory reported the chemical composition of ultrafiltered (0.1–60 μm) particulate matter at Station ALOHA. Their analysis included molecular biomarkers to constrain the sources of organic matter throughout the water column. Muramic acid, an amino sugar found only in the bacterial cell wall polymer peptidoglycan and D-amino acids (D-aspartic acid, D-glutamic acid, D-alanine, and D-serine) were used to estimate bacterial contributions to particulate matter (Kaiser and Benner, 2008; Kawasaki et al., 2011). Remarkably, C and N of bacterial origins accounted for ~30% (range 28-32%) of the total POC and \sim 50% (range 49-64%) of the particulate organic N (PON), the latter increasing with depth to >60% in the bathypelagic zone (Kaiser and Benner, 2008). It was estimated that <7% (deep) to 15% (surface) of the "bacterial biomass" was living bacteria; the remainder was particulate detritus of bacterial origin (Kaiser and Benner, 2008). However, comparisons of ultrafiltered particulate organic matter (0.1–60 μm) with ultrafiltered dissolved organic matter (1-100 nm) at Station ALOHA revealed a unique chemical composition for each fraction which argues against any simple aggregation-dissolution equilibrium between these two pools.

We have already established the fact that most of the PC in the water column, including the upper euphotic zone (0–100 m), is nonliving (Fig. 1a inset and Table 2). Yet the bulk molar PC:PN ratio is nearly identical to that of living cells; i.e., the canonical Redfield et al. (1963) ratio of 6.6. The average PC:PN in the 0–350 m region of the water column, which includes the entire euphotic zone (0–175 m) and the upper regions of the mesopelagic zone, is 6.7 (range 6.2–7.1) with the entire lower region of the euphotic zone (100–175 m) displaying PC:PN ratios that are even slightly lower than the Redfield ratio (Fig. 1b and Table 3). Furthermore, marine phytoplankton are thought to achieve Redfield stoichiometry only as they approach their maximum growth

rates (μ_{max}), and deviations from this optimum C:N ratio have been used to infer in situ growth rates (Goldman et al., 1979). Therefore, it may seem enigmatic that the large pool of particulate detritus appears to be in "stoichiometric equilibrium" with that of microorganisms growing at or near their maximal rates. Either the detrital pools of PC and PN are turning over at rates that coincidentally sustain the PC:PN ratios of nutrient-replete, rapidly growing cells, or some other process is acting to buffer the total particulate matter pool at the Redfield C:N ratio in the 0-350 m region of the water column, year round over the past 30 years. Only at depths \geq 500 m does the PC:PN ratio of the total particulate matter pools begin to deviate significantly from the Redfield ratio (Fig. 1b inset and Table 3). Similarly, the calcium carbonate corrected POC:PN molar ratio of sinking particulate matter collected in sediment traps deployed at 150 m averages 7.0 (Karl et al., 2021), indicating a stoichiometric coupling between production, recycling, and export of C and N at Station ALOHA.

Lee and Fuhrman (1987) measured C:N of bacteria grown in unamended, particle-free seawater cultures. They reported C:N weight ratios ranging from 2.5 to 4.3 with a mean of 3.7, equivalent to a C:N molar ratio of ~4.3. However, direct determinations of the C:N ratios of open ocean bacteria using either tangential flow filtration coupled to high temperature combustion (Fukuda et al., 1998) or transmission electron microscopy coupled to x-ray microanalysis (Gundersen et al., 2002) reported much higher C:N molar ratios (mean = 6.8, SD - 1.2 and geometric means of 5.3-9.1, respectively for the two independent studies). Average per cell C quotas for oceanic bacteria also appear to be much lower than the 20 fg C cell⁻¹ used by Lee and Fuhrman (1987). This is a critical point because Cho and Azam (1988) reported that 90% of all organic particulate matter in surface water was bacterial and that bacterial-C averaged ~70% of the total POC in the mesopelagic zone of the NPSG. These estimates are probably too high based on subsequent reports of the C cell quotas for oligotrophic oceanic bacteria, and on the ATP-based total microbial biomass-C estimates (an upper limit on bacterial biomass-C) presented herein.

It has been reported that, unlike C and N, particulate phosphorus (PP) in the surface waters of the NPSG is associated only with living organisms and, therefore, can be used as a "detritus-free biomass measurement" (Perry and Eppley, 1981). The authors employed a laboratory-derived PP:ATP weight (g g⁻¹) ratio of 6.6 to estimate living PP from field measurements of P-ATP in the Climax region of the NPSG, and compared that estimate of living P to direct measurements of PP. The median difference between the two estimates was 12% (Perry and Eppley, 1981). The authors concluded that PP must turn over much faster than PC or PN, following death by grazing or autolysis. This assumption of "P-free" particulate organic detritus has been invoked to identify geographically and stoichiometrically distinct plankton assemblages (Martiny et al., 2013). Nevertheless, growth rates estimated from ³³PO₄ uptake and PP concentrations indicated very low values (0.13–0.20 doublings d^{-1}) compared to the $\sim 1 d^{-1}$ from the PRPOOS and ADIOS field campaigns (Laws et al., 1984; Jones et al., 1996), indicative of the presence of nonliving PP. Indeed, it is well established that most of the particulate, P-containing deoxyribonucleic acid (DNA) in the sea is nonliving (Holm-Hansen et al., 1968; Sutcliffe et al., 1970; Winn and Karl, 1984), so the presence of PP in the detrital fraction seems to be well established. We estimated living PP at Station ALOHA for the period 2015-2018 using the previously employed weight ratio of 6.6 (Perry and Eppley, 1981) compared to our direct measurements of PP. In surface waters (0–75 m) where PP was fairly constant at \sim 0.5 µg P l⁻¹ (Hebel and Karl, 2001) and the mean P-ATP of \sim 30 ng l⁻¹ (Fig. 1a and Table 1), the PP:ATP relationship of Perry and Eppley (1981) predicts a biomass-P that equates to \sim 50% of the total PP pool. This value is higher than we report herein for PC (~30%; Table 2), but still far from the 100% estimate, as previously assumed.

Finally, Hernes and Benner (2002) reported a significant concentration of lignin phenols at Station ALOHA, biomarkers for terrigenous organic matter with no known marine source. A lignin concentration

peak for the 0.1–60 µm size class was observed at the depth corresponding to the North Pacific Intermediate Water, which for Station ALOHA is present from 500 to 800 m. Based on a two-end-member mixing model for organic matter with marine sources having a $\delta^{13}C=-22^\circ/_{00}$ and terrestrial sources a $\delta^{13}C=-27^\circ/_{00}$ and no fractionation, terrigenous organic matter at Station ALOHA was estimated to be 22–89% of the total POC, with an average of 70% at depths >100 m. Proposed sources include atmospheric deposition in the source waters near the Sea of Okhotsk, riverine input from the Kamchatka Peninsula and Siberia, or both (Hernes and Benner, 2002). It remains unknown whether any fraction of the mesopelagic P-ATP that we report herein is also supplied via horizontal transport to our study site. However, the possibility of terrigenous P-ATP at our study site seems highly unlikely, if not improbable.

4.5. Biomass distributions: energy and ecology

The earliest ecological application of the ATP assay was to determine the total microbial biomass profile in the sea, and to compare biomass distributions in space and time (Holm-Hansen and Booth, 1966; Holm-Hansen, 1969). Several general patterns emerged from these initial investigations, including decreases in P-ATP with distance from shore and with depth in the water column. Perhaps more importantly, the coastal enrichments in P-ATP were not just a surface phenomenon, but extended well into the mesopelagic zone. For example, in a neritic-to-oceanic transect off central California, the 5 ng P-ATP l⁻¹ isopleth depth decreased from ~1300 m near the coast to ~400 m in the open sea (Karl and Dobbs, 1998). It was concluded that the subeuphotic zone enrichment in P-ATP in the coastal region was a manifestation of a higher rate of near-surface primary production coupled to an increased flux of reduced carbon and energy in the form of sinking particulate matter (Karl and Dobbs, 1998). Consequently, an exponential decrease in particle flux (Knauer et al., 1979; Martin et al., 1987) would be expected to sustain an exponential decrease in total microbial biomass, if sinking particles were the primary source of nutrition (Cho and Azam, 1988).

At Station ALOHA, the mean water column inventory (0-4800 m) of P-ATP is 7.9 mg m⁻², of which 61% resides in depths >100 m, and 22% in the bathypelagic zone (>1000 m; Table 2). Our total water column microbial biomass estimate \sim 2 g C m $^{-2}$ (1.2 g C m $^{-2}$ > 100 m) is comparable to previous estimates of 1.9 g C m⁻² (200-4000 m) for the sum of prokaryotes (1.6 g m⁻²) plus HNF (0.3 g m⁻²) for samples collected on the global ocean Malaspina expedition (Pernice et al., 2015). Sohrin et al. (2010) reported an even larger microbial biomass for their three NPSG stations with a mean 100-4000 m estimate of 2.1 g C m^{-2} (prokaryotes = 1.9 g C m^{-2} , HNF = 0.2 g C m^{-2} , ciliates = 0.03 g C m⁻²). Consequently, our P-ATP-based estimate of 1.2 g C m⁻² for total microbial biomass for the >100 m portion of the water column is lower than the estimates based on microscopy and estimates of cell biovolume. The estimate reported by Yamaguchi et al. (2004) of 7.4 g C m⁻² for bacteria (4.7 g C m^{-2}) plus phytoplankton (1.1 g C m^{-2}) plus protozooplankton (1.6 g C m⁻²) for a station at 25°N, 137°E is unrealistically high and probably a result of their acknowledged use of "old" conversion factors, as discussed previously. So our conclusion that the majority of total water column microbial biomass-C is found at depths >100 m conforms to the limited previous reports. If sinking organic C supports the majority of living organisms below the euphotic zone, it is difficult to reconcile this observed biomass distribution, where more than half of the living microbial C is present at depths greater than the photosynthetic compensation depth (~175 m; Laws et al., 2014; Fig. 9).

Studies of mesopelagic and bathypelagic zone microbial respiration suggest that >70% of the carbon demand could be supplied by sinking particles (Arístegui et al., 2005). Furthermore, respiration has a very strong depth-dependence with mesopelagic zone (150–1000 m) rates of 3.4 mol C m $^{-2}$ yr $^{-1}$ compared to bathypelagic zone (>1000 m) rates of $\sim\!0.5$ mol C m $^{-2}$ yr $^{-1}$, again supporting a model where sinking particulate matter is the major supplier of organic C and energy to sustain

microbial metabolic processes. In the open ocean, direct measurements of microbial respiration by in vitro oxygen consumption are not possible at depths greater than $\sim\!200$ m (without pre-concentration of the sample) due to the limited sensitivity of the method. Consequently, indirect methods to estimate microbial respiration must be employed. Martin et al. (1987) used data on sinking particle flux attrition to constrain mesopelagic-bathypelagic oxygen utilization rates for several North Pacific Ocean stations. They reasoned that the vertical flux attrition of organic matter is due to the remineralization of organic matter and used estimates of 1.0, 1.5, and 0.25 mol of O_2 consumed per mole of C, N, and H atoms remineralized. Based on their open ocean composite C flux profile, subeuphotic oxygen utilization rates ranged from $\sim\!\!1$ mmol O_2 m $^{-3}$ yr $^{-1}$ at 500 m to < 0.1 mmol O_2 m $^{-3}$ yr $^{-1}$ at 2000 m (Martin et al., 1987).

The most frequently used approach is the measurement of respiratory Electron Transport System (ETS) dehydrogenase enzyme activity (Packard, 1971). This method relies on the extraction of the ETS enzymes from living microbes followed by in vitro measurement of its reduction of 2-p-iodophenyl-3-p-nitrophenyl-5-phenyltetrazolium chloride (INT) to formazan (reduced INT; INT-F) that is measured spectrophotometrically (Packard et al., 1971). Martínez-Garcia et al. (2009) adapted the INT method to provide measurements of in vivo rates during short-term incubations and applied a conversion factor of 12.8 mol O₂ consumed per mol INT-F produced, although the accuracy of this method has recently been called into question (Baños et al., 2020). The in vivo INT method was employed at Station ALOHA to estimate microbial respiration in the mesopelagic zone (200-1000 m) during a 1-yr period. Respiration rates varied with depth from an average of 107 µmol $O_2 \, m^{-3} \, d^{-\bar{1}}$ in the upper mesopelagic zone (200–350 m) to 56 μ mol O_2 $m^{-3} d^{-1}$, with a local maximum at 600-650 m (Martínez-Garcia, 2017), similar to local P-ATP concentration peaks described earlier. Size fractionation using Nuclepore® membranes revealed that the >0.8 μ m:0.2–0.8 μ m respiration ratio was \sim 1:1, suggesting an important role for larger (HNA) bacteria, free-living protists, or particle-associated microorganisms. Martínez-Garcia (2017) also reported seasonal variations in mesopelagic zone respiration, with higher summer rates associated with higher euphotic zone primary production and particle export, supporting the general model of Cho and Azam (1988) for contemporaneous epipelagic and mesopelagic zone coupling. However, the PC supply from the euphotic zone was not large enough to support mesopelagic zone respiration without an additional subsidy, based on the in vivo INT rate estimations. A similar imbalance was reported for Station ALOHA between estimates of bacterial and zooplankton respiration versus losses due to sinking POC (Steinberg et al., 2008). Their results indicated that the demand for C was ~5-fold greater than that supplied by particle export. The authors hypothesized that vertically migrating mesozooplankton might provide an organic C subsidy to the mesopelagic zone needed to sustain the estimated heterotrophic C demands. From an energetic viewpoint, these results are difficult to reconcile with our current understanding of trophodynamics. Sorokin (1971) postulated that mesopelagic zone microbial processes may be fueled not only by vertical fluxes of C and energy, but also by horizontal processes that import C and energy from more productive regions. While the importance of this horizontal transport hypothesis has been challenged (Banse, 1974), it cannot be rejected at this time.

At Station ALOHA, total depth-integrated P-ATP beneath the euphotic zone (150–4800 m) exceeds P-ATP in the 0–150 m region of the water column by $\sim\!25\%$ (Tables 1 and 2). If we assume that primary energy capture occurs exclusively in the euphotic zone via photosynthesis, and that <10% of the photosynthetically-derived carbon and energy is exported to the upper mesopelagic zone at 150 m (Grabowski et al., 2019), this permanent, inverted depth distribution of biomass-C based on measurements of P-ATP over a 30-yr period appears to be enigmatic. There must be a corresponding decrease in biomass-C production rate and total energy transformation with depth to sustain these microbial biomass distributions, especially throughout the mesopelagic

and bathypelagic zones. However, it has been reported that cell-specific prokaryotic production in the North Atlantic Ocean, estimated by ³Hleucine incorporation, is approximately constant (range 15-58 fmol C cell⁻¹ d⁻¹) throughout the water column to depths of 4000 m (Reinthaler et al., 2006). Based on estimated production and respiration rates (by the ETS method), the prokaryotic carbon demand was two orders of magnitude greater than the predicted (not measured) PC flux from the euphotic zone at two open ocean sites in the North Atlantic Ocean (Reinthaler et al., 2006). A similar, depth (0-900 m) invariant pattern of biomass-C (based on P-ATP measurements) specific DNA synthesis using ³H-adenine incorporation (Karl and Knauer, 1984b; Winn and Karl, 1984) was also reported more than two decades earlier in the North Pacific Ocean. A follow-on study confirmed that sinking PC contributed only 4–12% of the estimated prokaryotic C demand, leading to conclude that suspended particulate matter might be important in aphotic zone nutrition, with chemolithoautotrophic fixation of CO2 via oxidation of reduced inorganic substrates serving to replenish the deep water PC inventory (Baltar et al., 2010). However, net autotrophy in the mesopelagic and bathypelagic zones would require a supply of potential energy in the form of reduced substrates (e.g., ammonium, sulfide, hydrogen), the so-called reduced inorganic detrital electron flux (Karl and Knauer, 1984a). Since most reduced inorganic substances in the sea ultimately derive from energy initially captured during photosynthesis, the net production of organic carbon in the aphotic zone by the process of chemolithoautotrophy would be constrained, thermodynamically, by the coupled primary production - PC export processes. Extensive measurements of PC export at Station ALOHA indicate that the euphotic zone export ratio (e-ratio = PC export at 150 m \div 0-150 m depthintegrated ¹⁴C-based primary production) are <0.1 year round (Karl et al., 2003; Karl et al., 2021), and that the depth-dependent flux attrition in the mesopelagic zone is positively related to the export measured at 150 m (Church et al., 2021). Furthermore, the C supply versus C demand balance may be exacerbated by the fact that the C-specific enthalpy of organic matter decreases as particles age while sinking (Grabowski et al., 2019). Although particles leaving the euphotic zone were energy-replete based on measurements of C-normalized enthalpy (45–50 J mg⁻¹ POC), those captured at 500 m were relatively energydepleted (~11 J mg⁻¹ POC; Grabowski et al., 2019). The apparent imbalance between aphotic zone metabolic demand, and the supply of reduced carbon and energy may be reconciled purely by uncertainties in current measurements and conversion factors, or by invoking additional pathways and mechanisms of carbon and energy delivery to close the regional budgets (Burd et al., 2010). Regardless, microbial processes in the aphotic zone are fundamental to our understanding of the ocean's carbon cycle and, therefore, demand an improved understanding of some of these most basic processes (Arístegui et al., 2009; Herndl and Reinthaler, 2013).

5. Conclusions

In the sea, microorganisms are central to both the production and consumption of ATP and, therefore, sustain the oceanic ATP cycle. ATP provides the energy required for the metabolism and reproduction of growing cells, as well as for maintenance of viable, but nongrowing cells. ATP has such a central role in biology that Morowitz (1979) once lamented "one of these days a poet will appear to honor the molecule of ATP." So we propose the following Haiku:

ocean ATP microbial biomass foundation of life.

We present an extensive, 30-yr data set on microbial biomass and total PC at Station ALOHA in the NPSG. We observed an $\sim\!50$ -fold range in microbial biomass from the surface ocean to the abyss with average values of 8.3 mg C m $^{-3}$ to 0.1–0.2 mg C m $^{-3}$, respectively. We conclude

that the majority (70–97%) of the suspended PC pool is nonliving, regardless of season or depth. We document a large seasonal accumulation of organic detritus in the euphotic zone (0–175 m) that resets each winter. However, the PC:PN ratio of the bulk particulate matter pool does not change and appears to be in stoichiometric equilibrium with microbial biomass (C:N ~ 6.7) despite the large contributions of nonliving PC. A relatively short (<3 months) spring bloom was observed in the lower portion of the euphotic zone (125–150 m) during which both P-ATP and PC accumulate as a result of net growth on nutrients entrained into this region each winter. The mean water column inventory (0–4800 m) of P-ATP is 7.9 mg m $^{-2}$, of which 61% resides in depths >100 m, and 22% in the bathypelagic zone (>1000 m). We also present depth range-specific inventories of microbial biomass-C and discuss their origins and sources of carbon and energy required to sustain their distributions.

Finally, Deming et al. (1977) concluded that "the best interpretation of ATP data from natural samples requires a thorough knowledge of the microbial community structure and the environmental conditions," so in their opinion the ATP-biomass assay should be viewed as a complementary approach for understanding microbial processes in the marine environment. We concur with this assessment and, through our efforts in the HOT program, have endeavored to build a unique interdisciplinary field program that is poised for discovery in a sea of opportunity.

Disclosure

The research described herein is a collaboration of individuals who brought unique skills and talents to the project such that the whole is greater than the sum of its parts. DMK, MJC, and RML designed and defended the program over many review cycles, and worked to obtain extramural support. All co-authors conducted the study, led specific research components, and analyzed samples. Specifically, KMB and EMG led P-ATP and PC/PN analyses, respectively, and LAF developed and sustained the HOT-DOGS data system that is an invaluable asset for data distribution, analysis, and presentation. RML performed all statistical analyses. DMK wrote the first draft of the manuscript and all coauthors edited and improved several earlier versions. All authors consented to the article.

Declaration of Competing Interest

The authors declare that they have no known competing financial interests or personal relationships that could have appeared to influence the work reported in this paper.

Acknowledgements

We thank the many scientists, field and laboratory technicians, students, postdoctoral scholars, ships' officers and crew, and the HOT program support staff who have contributed to the success of the Hawaii Ocean Time-series (HOT) program since its inception in 1988. We also acknowledge the continuous financial support received from the National Science Foundation (current grant OCE-1756517; A.E. White, P. I.), and additional support from the Simons Foundation (SCOPE #329108 [DMK and MJC], #721252 [DMK], and #721221 [MJC]). This paper is dedicated to the memory of Osmund Holm-Hansen who pioneered the ATP-biomass assay and served as an influential mentor to DMK and RML.

Appendix A. Supplementary material

Supplementary data to this article can be found online at https://doi.org/10.1016/j.pocean.2022.102803.

References

- Altabet, M.A., 1990. Organic C, N, and stable isotopic composition of particulate matter collected on glass-fiber and aluminum oxide filters. Limnol. Oceanogr. 35 (4), 902–909. https://doi.org/10.4319/lo.1990.35.4.0902.
- Amy, P.S., Pauling, C., Morita, R.Y., 1983. Starvation-survival processes of a marine vibrio. Appl. Environ. Microbiol. 45 (3), 1041–1048.
- Arístegui, J., Agustí, S., Middelburg, J.J., Duarte, C.M., 2005. Respiration in the mesopelagic and bathypelagic zones of the ocean. In: del Giorgio, P.A., Williams, P.J. LeB (Eds.), Respiration in Aquatic Ecosystems. Oxford Univ. Press, New York, NY, pp. 181–205.
- Arístegui, J., Gasol, J.M., Duarte, C.M., Herndl, G.J., 2009. Microbial oceanography of the dark ocean's pelagic realm. Limnol. Oceanogr. 54 (5), 1501–1529. https://doi. org/10.4319/lo.2009.54.5.1501.
- Azam, F., Hodson, R.E., 1977. Dissolved ATP in the sea and its utilisation by marine bacteria. Nature 267 (5613), 696–698. https://doi.org/10.1038/267696a0.
- Azam, F., Beers, J.R., Campbell, L., Carlucci, A.F., Holm-Hansen, O., Reid, F.M.H., Karl, D.M., 1979. Occurrence and metabolic activity of organisms under the Ross Ice Shelf, Antarctica, at Station J9. Science 203 (4379), 451–453. https://doi.org/10.1126/science.203.4379.3451
- Baltar, F., Arístegui, J., Sintes, E., Gasol, J.M., Reinthaler, T., Herndl, G.J., 2010. Significance of non-sinking particulate organic carbon and dark CO₂ fixation to heterotrophic carbon demand in the mesopelagic northeast Atlantic. Geophys. Res. Lett. 37 (9), L09602. https://doi.org/10.1029/2010GL043105.
- Baños, I., Montero, M.F., Benavides, M., Arístegui, J., 2020. INT toxicity over natural bacterial assemblages from surface oligotrophic waters: Implications for the assessment of respiratory activity. Microb. Ecol. 80 (1), 237–242. https://doi.org/ 10.1007/s00248-019-01479-4.
- Banse, K., 1974. On the role of bacterioplankton in the tropical ocean. Mar. Biol. 24 (1), 1–5. https://doi.org/10.1007/BF00402841.
- Barone, B., Bidigare, R.R., Church, M.J., Karl, D.M., Letelier, R.M., White, A.E., 2015. Particle distributions and dynamics in the euphotic zone of the North Pacific Subtropical Gyre. J. Geophys. Res. - Oceans 120 (5), 3229–3247. https://doi.org/ 10.1002/2015.10010774.
- Barone, B., Nicholson, D.P., Ferrón, S., Firing, E., Karl, D.M., 2019. The estimation of gross oxygen production and community respiration from autonomous time-series measurements in the oligotrophic ocean. Limnol. Oceanogr. Meth. 17 (12), 650–664. https://doi.org/10.1002/lom3.10340.
- Beers, J.R., Reid, F.M.H., Stewart, G.L., 1975. Microplankton of the North Pacific central gyre. Population structure and abundance, June 1973. Int. Revue ges. Hydrobiol. 60 (5) 607–638
- Beers, J.R., Reid, F.M.H., Stewart, G.L., 1982. Seasonal abundance of the microplankton population in the North Pacific central gyre. Deep-Sea Res. Pt. A 29 (2), 227–245. https://doi.org/10.1016/0198-0149(82)90111-X.
- Benner, R., Kaiser, K., 2003. Abundance of amino sugars and peptidoglycan in marine particulate and dissolved organic matter. Limnol. Oceanogr. 48 (1), 118–128. https://doi.org/10.4319/lo.2003.48.1.0118.
- Björkman, K.M., Karl, D.M., 2005. Presence of dissolved nucleotides in the North Pacific Subtropical Gyre and their role in cycling of dissolved organic phosphorus. Aquat. Microb. Ecol. 39 (2), 193–203. https://doi.org/10.3354/ame039193.
- Björkman, K., Thomson-Bulldis, A.L., Karl, D.M., 2000. Phosphorus dynamics in the North Pacific subtropical gyre. Aquat. Microb. Ecol. 22 (2), 185–198. https://doi. org/10.3354/ame022185.
- Bochdansky, A.B., Stouffer, A.N., Washington, N.N., 2021. Adenosine triphosphate (ATP) as a metric of microbial biomass in aquatic systems: new simplified protocols, laboratory validation, and a reflection on data from the literature. Limnol. Oceanogr. Meth. 19 (2), 115–131. https://doi.org/10.1002/lom3.10409.
- Burd, A.B., Hansell, D.A., Steinberg, D.K., Anderson, T.R., Arístegui, J., Baltar, F., Beaupré, S.R., Buesseler, K.O., DeHairs, F., Jackson, G.A., Kadko, D.C., Koppelmann, R., Lampitt, R.S., Nagata, T., Reinthaler, T., Robinson, C., Robison, B. H., Tamburini, C., Tanaka, T., 2010. Assessing the appraent imbalance between geochemical and biochemical indicators of meso- and bathypelagic biological activity: What the @\$#! is wrong with present calculations of carbon budgets? Deep-Sea Res. Pt. II 57 (16), 1557–1571. https://doi.org/10.1016/j.dsr2.2010.02.022.
- Campbell, L., Nolla, H.A., Vaulot, D., 1994. The importance of *Prochlorococcus* to community structure in the central North Pacific Ocean. Limnol. Oceanogr. 39 (4), 954–961. https://doi.org/10.4319/lo.1994.39.4.0954.
- Casey, J.R., Aucan, J.P., Goldberg, S.R., Lomas, M.W., 2013. Changes in partitioning of carbon amongst photosynthetic pico- and nano-plankton groups in the Sargasso Sea in response to changes in the North Atlantic Oscillation. Deep-Sea Res. Pt. II 93, 58–70. https://doi.org/10.1016/j.dsr2.2013.02.002.
- Casey, J.R., Björkman, K.M., Ferrón, S., Karl, D.M., 2019. Size dependence of metabolism within marine picoplankton populations. Limnol. Oceanogr. 64 (4), 1819–1827. https://doi.org/10.1002/lno.11153.
- Chapman, A.G., Atkinson, D.E., 1977. Adenine nucleotide concentrations and turnover rates. Their correlation with biological activity in bacteria and yeast. Adv. Microb. Physiol. 15, 253–306. https://doi.org/10.1016/S0065-2911(08)60318-5.
- Cho, B.C., Azam, F., 1988. Major role of bacteria in biogeochemical fluxes in the ocean's interior. Nature 332 (6163), 441–443. https://doi.org/10.1038/332441a0.
- Christian, J.R., Karl, D.M., 1994. Microbial community structure at the U.S.-Joint Global Ocean Flux Study Station ALOHA: inverse methods for estimating biochemical indicator ratios. J. Geophys. Res. Oceans 99 (C7), 14269–14276. https://doi.org/ 10.1029/94JC00681.
- Church, M.J., Wai, B., Karl, D.M., DeLong, E.F., 2010. Abundances of crenarchaeal amoA genes and transcripts in the Pacific Ocean. Environ. Microbiol. 12 (3), 679–688. https://doi.org/10.1111/j.1462-2920.2009.02108.x.

- Church, M., Kyi, E., Hall, B., Karl, D., Lindh, M., Nelson, A., Wear, E., 2021. Production and diversity of microorganisms associated with sinking particles in the subtropical North Pacific Ocean. Limnol. Oceanogr. 66 (9), 3255–3270. https://doi.org/ 10.1002/jno.11877.
- Daley, R.J., 1979. Direct epifluorescence enumeration of native aquatic bacteria: uses, limitations, and comparative accuracy. In: Costerton, J.W., Colwell, R.R. (Eds.), Native Aquatic Bacteria: Enumeration, Activity and Ecology. ASTM International, West Conshohocken, PA, pp. 29–45.
- Dawes, E.A., Large, P.J., 1970. Effect of starvation on the viability and cellular constituents of *Zymomonas anaerobia* and *Zymomonas mobilis*. J. Gen. Microbiol. 60 (1), 31–42. https://doi.org/10.1099/00221287-60-1-31.
- DeLong, E.F., 1992. Archaea in coastal marine environments. Proc. Natl. Acad. Sci. USA 89 (12), 5685–5689. https://doi.org/10.1073/pnas.89.12.5685.
- Deming, J.W., Picciolo, G.L., Chappelle, E.W., 1977. Important factors in adenosine triphosphate determinations using firefly luciferase: applicability of the assay to studies of native aquatic bacteria. In: Costerton, J.W., Colwell, R.R. (Eds.), Native Aquatic Bacteria: Enumeration, Activity, and Ecology. American Society for Testing and Materials, Philadelphia, PA, pp. 89–98.
- Dore, J.E., Letelier, R.M., Church, M.J., Lukas, R., Karl, D.M., 2008. Summer phytoplankton blooms in the oligotrophic North Pacific Subtropical Gyre: historical perspective and recent observations. Prog. Oceanogr. 76 (1), 2–38. https://doi.org/ 10.1016/j.pocean.2007.10.002.
- Eppley, R.W., 1982. The PRPOOS program: a study of plankton rate processes in oligotrophic oceans. Eos, Trans. Amer. Geophys. Un. 63 (22), 522. https://doi.org/ 10.1029/E0063i022n00522-01.
- Eppley, R.W., Carlucci, A.F., Holm-Hansen, O., Kiefer, D., McCarthy, J.J., Venrick, E., Williams, P.M., 1971. Phytoplankton growth and composition in shipboard cultures supplied with nitrate, ammonium, or urea as the nitrogen source. Limnol. Oceanogr. 16 (5), 741–751. https://doi.org/10.4319/lo.1971.16.5.0741.
- Eppley, R.W., Renger, E.H., Venrick, E.L., Mullin, M.M., 1973. A study of plankton dynamics and nutrient cycling in the central gyre of the North Pacific Ocean. Limnol. Oceanogr. 18 (4), 534–551. https://doi.org/10.4319/lo.1973.18.4.0534.
- Eppley, R.W., Harrison, W.G., Chisholm, S.W., Stewart, E., 1977. Particulate organic matter in surface waters off southern California and its relation to phytoplankton. J. Mar. Res. 35 (4), 671–696.
- Fellows, D.A., Karl, D.M., Knauer, G.A., 1981. Large particle fluxes and the vertical transport of living carbon in the upper 1500 m of the northeast Pacific Ocean. Deep-Sea Res. Pt. A 28 (9), 921–936. https://doi.org/10.1016/0198-0149(81)90010-8.
- Fournier, R.O., 1966. North Atlantic deep-sea fertility. Science 153 (3741), 1250–1252. https://doi.org/10.1126/science.153.3741.1250.
- Fournier, R.O., 1970. Studies on pigmented microorganisms from aphotic marine environments. Limnol. Oceanogr. 15 (5), 675–682. https://doi.org/10.4319/lo.1970.15.5.0675.
- Fournier, R.O., 1971. Studies on pigmented microorganisms from aphotic marine environments. II. North Atlantic distribution. Limnol. Oceanogr. 16 (6), 952–961. https://doi.org/10.4319/10.1971.16.6.0952.
- Fournier, R.O., 1973. Studies on pigmented microorganisms from aphotic marine environments. III. Evidence of apparent utilization by benthic and pelagic tunicata. Limnol. Oceanogr. 18 (1), 38–43. https://doi.org/10.4319/lo.1973.18.1.0038.
- Fuhrman, J.A., McCallum, K., Davis, A.A., 1992. Novel major archaebacterial group from marine plankton. Nature 356 (6365), 148–149. https://doi.org/10.1038/356148a0.
- Fukuda, R., Ogawa, H., Nagata, T., Koike, I., 1998. Direct determination of carbon and nitrogen contents of natural bacterial assemblages in marine environments. Appl. Environ. Microbiol. 64 (9), 3352–3358. https://doi.org/10.1128/AEM.64.9.3352-3358 1008
- Gasol, J.M., del Giorgio, P.A., Duarte, C.M., 1997. Biomass distribution in marine planktonic communities. Limnol. Oceanogr. 42 (6), 1353–1363. https://doi.org/ 10.4319/lo.1997.42.6.1353
- Goldman, J.C., McCarthy, J.J., Peavey, D.G., 1979. Growth rate influence on the chemical composition of phytoplankton in oceanic waters. Nature 279 (5710), 210–215. https://doi.org/10.1038/279210a0.
- Gordon, D.C., Jr., 1970. Chemical and biological observations at Station Gollum, an oceanic station near Hawaii, January 1969 to June 1970. HIG-70-22, 44 pages.
- Gordon Jr., D.C., 1971. Distribution of particulate organic carbon and nitrogen at an oceanic station in the central Pacific. Deep-Sea Res. Oceanogr. Abstr. 18 (11), 1127–1134. https://doi.org/10.1016/0011-7471(71)90098-2.
- Gowing, M.M., Silver, M.W., 1985. Minipellets: a new and abundant size class of marine fecal pellets. J. Mar. Res. 43 (2), 395–418. https://doi.org/10.1357/ 002224085788438676.
- Grabowski, E., Letelier, R.M., Laws, E.A., Karl, D.M., 2019. Coupling carbon and energy fluxes in the North Pacific Subtropical Gyre. Nat. Commun. 10 (1), 1–9. https://doi. org/10.1038/s41467-019-09772-z.
- Grubbs, F.E., 1969. Procedures for detecting outlying observations in samples. Technometrics 11 (1), 1–21. https://doi.org/10.1080/00401706.1969.10490657.
- Gundersen, K., Heldal, M., Norland, S., Purdie, D.A., Knap, A.H., 2002. Elemental C, N, and P cell content of individual bacteria collected at the Bermuda Atlantic Timeseries Study (BATS) site. Limnol. Oceanogr. 47 (5), 1525–1530. https://doi.org/10.4319/lo.2002.47.5.1525.
- Hamilton, R.D., Holm-Hansen, O., Strickland, J.D.H., 1968. Notes on the occurrence of living microscopic organisms in deep water. Deep-Sea Res. Oceanogr. Abstr. 15 (6), 651–656.
- Hebel, D.V., Karl, D.M., 2001. Seasonal, interannual and decadal variations in particulate matter concentrations and composition in the subtropical North Pacific Ocean. Deep-Sea Res. Pt. II 48 (8), 1669–1695. https://doi.org/10.1016/S0967-0645(00)00155-

- Henderikx-Freitas, F., Karl, D.M., Björkman, K., White, A.E., 2021. Constraining growth rates and the ratio of living to nonliving particulate carbon using beam attenuation and adenosine-5-triphosphate at Station ALOHA. Limnol. Oceanogr. Lett 6 (5), 243–252. https://doi.org/10.1002/lol2.10199.
- Hentschel, E., 1936. Allgemeine Biologie des Südatlantischen Ozeans. Wiss. Ergeb. Deut. Atl. Exped. Meteor 1925–1927 (11), 1–344.
- Herndl, G.J., Reinthaler, T., 2013. Microbial control of the dark end of the biological pump. Nature Geosci. 6 (9), 718–724. https://doi.org/10.1038/ngeo1921.
- Herndl, G.J., Reinthaler, T., Teira, E., van Aken, H., Veth, C., Pernthaler, A., Pernthaler, J., 2005. Contribution of Archaea to total prokaryotic production in the deep Atlantic Ocean. Appl. Environ. Microbiol. 71 (5), 2303–2309. https://doi.org/ 10.1128/AEM.71.5.2303-2309.2005.
- Hernes, P.J., Benner, R., 2002. Transport and diagenesis of dissolved and particulate terrigenous organic matter in the North Pacific Ocean. Deep-Sea Res. Pt. I 49 (12), 2119–2132. https://doi.org/10.1016/S0967-0637(02)00128-0.
- Hobbie, J.E., Daley, R.J., Jasper, S., 1977. Use of Nuclepore filters for counting bacteria by fluorescence microscopy. Appl. Environ. Microbiol. 33 (5), 1225–1228. https://doi.org/10.1128/AEM.33.5.1225-1228.1977.
- Hodson, R.E., Azam, F., Carlucci, A.F., Fuhrman, J.A., Karl, D.M., Holm-Hansen, O., 1981. Microbial uptake of dissolved organic matter in McMurdo Sound. Antarctica. Mar. Biol. 61 (2–3), 89–94. https://doi.org/10.1007/BF00386648.
- Holm-Hansen, O., 1969. Determination of microbial biomass in ocean profiles. Limnol. Oceanogr. 14 (5), 740–747. https://doi.org/10.4319/lo.1969.14.5.0740.
- Holm-Hansen, O., 1970a. ATP levels in algal cells as influenced by environmental conditions. Plant Cell Physiol. 11 (5), 689–700. https://doi.org/10.1093/ oxfordjournals.pcp.a074557.
- Holm-Hansen, O., 1970b. Determination of microbial biomass in deep ocean water. In: Hood, D. (Ed.), Organic Matter in Natural Waters. Institute of Marine Science, Fairbanks, AK, pp. 287–300.
- Holm-Hansen, O., 1973. Determination of total microbial biomass by measurement of adenosine triphosphate. In: Stevenson, L.H., Colwell, R.R. (Eds.), Estuarine Microbial Ecology. University of South Carolina Press, Columbia, SC, pp. 73–89.
- Holm-Hansen, O., Booth, C.R., 1966. The measurement of adenosine triphosphate in the ocean and its ecological significance. Limnol. Oceanogr. 11 (4), 510–519. https:// doi.org/10.4319/lo.1966.11.4.0510.
- Holm-Hansen, O., Paerl, H.W., 1972. The applicability of ATP determination for estimation of microbial biomass and metabolic activity. Mem. Ist. Ital. Idrobiol. Dott. Marco de Marchi 29 (Suppl), 149–168.
- Holm-Hansen, O., Sutcliffe Jr., W.H., Sharp, J., 1968. Measurement of deoxyribonucleic acid in the ocean and its ecological significance. Limnol. Oceanogr. 13 (3), 507–514. https://doi.org/10.4319/lo.1968.13.3.0507.
- Holm-Hansen, O., Mitchell, B.G., Hewes, C.D., Karl, D.M., 1989. Phytoplankton blooms in the vicinity of Palmer Station. Antarctica. Polar Biol. 10 (1), 49–57. https://doi. org/10.1007/BF00238290.
- Jannasch, H.W., Jones, G.A., 1959. Bacterial populations in sea water as determined by different methods of enumeration. Limnol. Oceanogr. 4 (2), 128–139.
- Jones, D.R., Karl, D.M., Laws, E.A., 1996. Growth rates and production of heterotrophic bacteria and phytoplankton in the North Pacific subtropical gyre. Deep-Sea Res. Pt. I 43 (10), 1567–1580. https://doi.org/10.1016/S0967-0637(96)00079-9.
- Kaiser, K., Benner, R., 2008. Major bacterial contribution to the ocean reservoir of detrital organic carbon and nitrogen. Limnol. Oceanogr. 53 (3), 99–112. https://doi. org/10.4319/lo.2008.53.1.0099.
- Karl, D.M., 1978. Occurrence and ecological significance of GTP in the ocean and in microbial cells. Appl. Environ. Microbiol. 36 (2), 349–355.
- Karl, D.M., 1979. Adenosine triphosphate and guanosine triphosphate determinations in intertidal sediments. In: Litchfield, C.D., Seyfried, P.L. (Eds.), Methodology for Biomass Determinations and Microbial Activities in Sediments. ASTM International, West Conshohocken, PA, pp. 5–20.
- Karl, D.M., 1980. Cellular nucleotide measurements and applications in microbial ecology. Microbiol. Rev. 44 (4), 739–796. https://doi.org/10.1128/ MMBR 44 4 739-796. 1980
- Karl, D.M., 2007. Microbial nucleotide fingerprints in nature. In: Reddy, C.A., Beveridge, T., Breznak, J.A., Marzluf, G.A., Schmidt, T.M., Snyder, L.R. (Eds.), Methods for General and Molecular Microbiology. ASM Press, Washington, pp. 869–878. https://doi.org/10.1128/9781555817497.ch37.
- Karl, D.M., Dobbs, F.C., 1998. Molecular approaches to microbial biomass estimation in the sea. In: Cooksey, K.E. (Ed.), Molecular Approaches to the Study of the Ocean. Springer, Netherlands, pp. 29–89. https://doi.org/10.1007/978-94-011-4928-0_2.
- Karl, D.M., Holm-Hansen, O., 1978. Methodology and measurement of adenylate energy charge ratios in environmental samples. Mar. Biol. 48 (2), 185–197. https://doi.org/ 10.1007/BF00395018.
- Karl, D.M., Knauer, G.A., 1984a. Detritus-Microbe interactions in the marine pelagic environment: selected results from the VERTEX experiment. Bull. Mar. Sci. 35 (3), 550 EEG.
- Karl, D.M., Knauer, G.A., 1984b. Vertical distribution, transport, and exchange of carbon in the northeast Pacific Ocean: evidence for multiple zones of biological activity. Deep-Sea Res. Pt. A 31 (3), 221–243. https://doi.org/10.1016/0198-0149(84)
- Karl, D.M., Lukas, R., 1996. The Hawaii Ocean Time-series (HOT) Program: background, rationale and field implementation. Deep-Sea Res Pt. II 43 (2), 129–156. https://doi. org/10.1016/0967-0645(96)00005-7.
- Karl, D.M., Tien, G., 1997. Temporal variability in dissolved phosphorus concentrations in the subtropical North Pacific Ocean. Mar. Chem. 56 (1), 77–96. https://doi.org/ 10.1016/S0304-4203(96)00081-3.

- Karl, D.M., Winn, C.D., 1984. Adenine metabolism and nucleic acid synthesis: Applications to microbiological oceanography. In: Hobbie, J.E., Williams, P.J. le B. (Eds.), Heterotrophic Activity in the Sea. Plenum Press, New York, NY, pp. 197-215.
- Karl, D.M., LaRock, P.A., Morse, J.W., Sturges, W., 1976. Adenosine triphosphate in the North Atlantic Ocean and its relationship to the oxygen minimum. Deep-Sea Res. Oceanogr. Abstr. 23 (1), 81-88. https://doi.org/10.1016/0011-7471(76)90810-X.
- Karl, D.M., Burns, D.J., Orrett, K., Jannasch, H.W., 1984. Thermophilic microbial activity in samples from deep-sea hydrothermal vents. Mar. Biol. Lett. 5 (4), 227-231.
- Karl, D.M., Holm-Hansen, O., Taylor, G.T., Tien, G., Bird, D.F., 1991. Microbial biomass and productivity in the western Bransfield Strait, Antarctica during the 1986-87 austral summer. Deep-Sea Res. Pt. A 38 (8), 1029-1055. https://d
- Karl, D.M., Letelier, R., Hebel, D., Tupas, L., Dore, J., Christian, J., Winn, C., 1995. Ecosystem changes in the North Pacific subtropical gyre attributed to the 1991-92 El Niño, Nature 373 (6511), 230-234, https://doi.org/
- Karl, D.M., Björkman, K.M., Dore, J.E., Fujieki, L., Hebel, D.V., Houlihan, T., Letelier, R. M., Tupas, L.M., 2001. Ecological nitrogen-to-phosphorus stoichiometry at Station ALOHA. Deep-Sea Res. Pt. II 48 (8), 1529-1566. https://doi.org/10.1016/S0967-
- Karl, D.M., Bidigare, R.R., Letelier, R.M., 2002. Sustained and aperiodic variability in organic matter production and phototrophic microbial community structure in the North Pacific Subtropical Gyre. In: Williams, P.J.l.B., Thomas, D.N., Reynolds, C.S. (Eds.), Phytoplankton Productivity. Blackwell Science Ltd, Oxford, UK, pp. 222–264.
- Karl, D.M., Bates, N.R., Emerson, S., Harrison, P.J., Jeandel, C., Llinas, O., Liu, K.-K., Marty, J.-C., Michaels, A.F., Miquel, J.C., Neuer, S., Nojiri, Y., Wong, C.S., 2003. Temporal studies of biogeochemical processes determined from ocean time-series observations during the JGOFS era. In: Fasham, M.J.R. (Ed.), Ocean Biogeochemistry: The Role of the Ocean Carbon Cycle in Global Change. Springer-Verlag, New York, pp. 239-267. https://doi.org/10.1007/978-3-642-55844-3_11.
- Karl, D.M., Letelier, R.M., Bidigare, R.R., Björkman, K.M., Church, M.J., Dore, J.E., White, A.E., 2021. Seasonal-to-decadal scale variability in primary production and particulate matter export at Station ALOHA. Prog. Oceanogr. 195, 102563. https:// doi.org/10.1016/j.pocean.2021.102563.
- Karner, M.B., DeLong, E.F., Karl, D.M., 2001. Archaeal dominance in the mesopelagic zone of the Pacific Ocean. Nature 409 (6819), 507-510. https://doi.org/10.1038/
- Kawasaki, N., Sohrin, R., Ogawa, H., Nagata, T., Benner, R., 2011. Bacterial carbon content and the living and detrital bacterial contributions to suspended particulate organic carbon in the North Pacific Ocean. Aquat. Microb. Ecol. 62 (2), 165-176. https://doi.org/10.3354/ame01462.
- Keeling, C.D., Brix, H., Gruber, N., 2004. Seasonal and long-term dynamics of upper ocean carbon cycle at Station ALOHA near Hawaii, Glob, Biogeochem, Cv. 18 (4), GB4006. https://doi.org/10.1029/2004GB002227.
- Knauer, G.A., Martin, J.H., Bruland, K.W., 1979. Fluxes of particulate carbon, nitrogen, and phosphorus in the upper water column of the northeast Pacific. Deep-Sea Res. Pt. A 26 (8), 97–108. https://doi.org/10.1016/0198-0149(79)90089-X. Koenings, J.P., Hooper, F.F., 1973. Organic phosphorus compounds of a northern
- Michigan bog, bog-lake system. Mich. Acad. 5 (3), 295–310.
- Laws, E., 1984. Improved estimates of phytoplankton carbon based on ¹⁴C incorporation into chlorophyll a, J. Theor. Biol. 110 (3), 425–434. https://doi.org/10.1016/
- Laws, E.A., Karl, D.M., Redalje, D.G., Jurick, R.S., Winn, C.D., 1983. Variability in ratios of phytoplankton carbon and RNA to ATP and chlorophyll a in batch and continuous cultures. J. Phycol. 19 (4), 439-445. https://doi.org/10.1111/j.0022
- Laws, E.A., Redalje, D.G., Haas, L.W., Bienfang, P.K., Eppley, R.W., Harrison, W.G., Karl, D.M., Marra, J., 1984. High phytoplankton growth and production rates in oligotrophic Hawaiian coastal waters. Limnol. Oceanogr. 29 (6), 1161-1169. https://doi.org/10.4319/lo.1984.29.6.1161.
- Laws, E.A., Letelier, R.M., Karl, D.M., 2014. Estimating the compensation irradiance in the ocean: The importance of accounting for non-photosynthetic uptake of inorganic carbon. Deep-Sea Res. Pt. I 93, 35-40. https://doi.org/10.1016/j.dsr.2014.07.011.
- Lee, S., Fuhrman, J.A., 1987. Relationships between biovolume and biomass of naturally derived marine bacterioplankton. Appl. Environ. Microbiol. 53 (6), 1298-1303. https://doi.org/10.1128/AEM.53.6.1298-1303.1987
- Letelier, R.M., Dore, J.E., Winn, C.D., Karl, D.M., 1996. Seasonal and interannual variations in photosynthetic carbon assimilation at Station ALOHA. Deep-Sea Res. Pt. II 43 (2-3), 467-490. https://doi.org/10.1016/0967-0645(96)00006-9.
- Letelier, R.M., Karl, D.M., Abbott, M.R., Bidigare, R.R., 2004. Light driven seasonal patterns of chlorophyll and nitrate in the lower euphotic zone of the North Pacific Subtropical Gyre. Limnol. Oceanogr. 49 (2), 508-519. https://doi.org/10.4319/
- Letelier, R.M., Björkman, K.M., Church, M.J., Hamilton, D.S., Mahowald, N.M., Scanza, R.A., Schneider, N., White, A.E., Karl, D.M., 2019. Climate-driven oscillation of phosphorus and iron limitation in the North Pacific Subtropical Gyre. Proc. Natl. Acad. Sci. USA 116 (26), 12720-12728. https://doi.org/10.1073/pnas.1900789116.
- Levin, G.V., Heim, A.H., 1965. Gulliver and Diogenes-exobiological antitheses. Life Sci. Space Res. 3, 105-119.
- Levin, G.V., Straat, P.A., 2016. The case for extant life on Mars and its possible detection by the Viking labeled release experiment. Astrobiol. 16 (10), 798-810. https://doi. org/10.1089/ast.2015.1464.
- Levin, G.V., Heim, A.H., Clendenning, J.R., Thompson, M.-F., 1962. Gulliver" A quest for life on Mars. Science 138 (3537), 114-121.
- Levin, G.V., Clendenning, J.R., Chappelle, E.W., Heim, A.H., Rocek, E., 1964. A rapid method for detection of microorganisms by ATP assay; its possible application in virus and cancer studies. BioScience 14 (4), 37-38.

- Lipmann, F., 1941. Metabolic generation and utilization of phosphate bond energy. In: Nord, F.F., Werkman, C.H. (Eds.), Advances in Enzymology and Related Areas of Molecular Biology, vol. 1. John Wiley & Sons Inc, Hoboken, NJ, pp. 99-162. https:// doi.org/10.1002/9780470122464.ch4.
- Liu, X., Levine, N.M., 2021. Ecosystem implications of fine-scale frontal disturbances in the oligotrophic ocean - An idealized modeling approach. Prog. Oceanogr. 192, 102519. https://doi.org/10.1016/j.pocean.2021.102519
- Lund, J.W.G., Kipling, C., LeCren, E.D., 1958. The inverted microscope method of estimating numbers and the statistical basis of estimations by counting. Hydrobiol. 11 (2), 143-170. https://doi.org/10.1007/BF00007865
- Martin, J.H., Knauer, G.A., Karl, D.M., Broenkow, W.W., 1987. VERTEX: carbon cycling in the northeast Pacific. Deep-Sea Res. Pt. A 34 (2), 267-285. https://doi.org/
- Martínez-Garcia, S., 2017. Microbial respiration in the mesopelagic zone at Station ALOHA. Limnol. Oceanogr. 62 (1), 320-333. https://doi.org/10.1002/lno.10397.
- Martínez-Garcia, S., Fernández, E., Aranguren-Gassis, M., Teira, E., 2009. In vivo electron transport system activity: a method to estimate respiration in natural marine microbial planktonic communities. Limnol. Oceanogr. Meth. 7 (6), 459-469. https://doi.org/10.4319/lom.2009.7.459.
- Martiny, A.C., Pham, C.T.A., Primeau, F.W., Vrugt, J.A., Moore, J.K., Levin, S.A., Lomas, M.W., 2013. Strong latitudinal patterns in the elemental ratios of marine plankton and organic matter. Nat. Geosci. 6 (4), 279-283. https://doi.org/10.1038/ ngeo1757
- McAndrew, P.M., Björkman, K.M., Church, M.J., Morris, P.J., Jachowski, N., Williams PJ, leB, Karl, D.M., 2007. Metabolic response of oligotrophic plankton communities to deep water nutrient enrichment. Mar. Ecol. Prog. Ser. 332, 63-75.
- McCarthy, M.D., Hedges, J.I., Benner, R., 1998. Major bacterial contribution to marine dissolved organic nitrogen. Science 281 (5374), 231-234. https://doi.org/10.1126/
- McElroy, W.D., 1947. The energy source for bioluminescence in an isolated system. Proc. Natl. Acad. Sci. USA 33 (11), 342–345. https://doi.org/10.1073/pnas.33
- Menden-Deuer, S., Lessard, E.J., 2000. Carbon to volume relationships for dinoflagellates, diatoms, and other protist plankton. Limnol. Oceanogr. 45 (3), 569-579. https://doi.org/10.4319/lo.2000.45.3.0569.
- Morgan-Smith, D., Herndl, G.J., van Aken, H.M., Bochdansky, A.B., 2011. Abundance of eukaryotic microbes in the deep subtropical North Atlantic. Aquat. Microb. Ecol. 65 (2), 103-115, https://doi.org/10.3354/ame1536
- Morgan-Smith, D., Clouse, M.A., Herndl, G.J., Bochdansky, A.B., 2013. Diversity and distribution of microbial eukaryotes in the deep tropical and subtropical North Atlantic Ocean. Deep-Sea Res. Pt. I 78, 58-69. https://doi.org/10.1016/j. dsr.2013.04.010.
- Morowitz, H.J., 1979. Bay to breakers. In: The Wine of Life and Other Essays on Societies, Energy and Living Things. St. Martin's Press, New York, NY, pp. 18-21.
- Nagata, T., Fukuda, H., Fukuda, R., Koike, I., 2000. Bacterioplankton distribution and production in deep Pacific waters: Large-scale geographic variations and possible coupling with sinking particles fluxes. Limnol. Oceanogr. 45 (2), 426-435. https:// doi.org/10.4319/lo.2000.45.2.0426.
- Nawrocki, M.P., Karl, D.M., 1989. Dissolved ATP turnover in the Bransfield Strait, Antarctica during a spring bloom. Mar. Ecol. Prog. Ser. 57 (1), 35–44. Newell, S.Y., Fallon, R.D., Tabor, P.S., 1986. Direct microscopy of natural assemblages.
- In: Poindexter, J.S., Leadbetter, E.R. (Eds.), Bacteria in Nature, Volume 2. Plenum Publishing Corp, New York, NY, pp. 1–48.
- Nicholson, D.P., Wilson, S.T., Doney, S.C., Karl, D.M., 2015. Quantifying subtropical North Pacific gyre mixed layer primary productivity from Seaglider observations of diel oxygen cycles. Geophys. Res. Lett. 42 (10), 4032-4039. https://doi.org/ /2015GL063065
- Pachiadaki, M.G., Sintes, E., Bergauer, K., Brown, J.M., Record, N.R., Swan, B.K., Mathyer, M.E., Hallam, S.J., Lopez-Garcia, P., Takaki, Y., Nunoura, T., Woyke, T., Herndl, G.J., Stepanauskas, R., 2017. Major role of nitrite-oxidizing bacteria in dark ocean carbon fixation. Science 358 (6366), 1046-1051. https://doi.org/10.1126/ science.aan8260.
- Packard, T.T., 1971. The measurement of respiratory electron-transport activity in marine phytoplankton. J. Mar. Res. 29 (3), 235-244.
- Packard, T.T., Healy, M.L., Richards, F.A., 1971. Vertical distribution of the activity of the respiratory electron transport system in marine plankton. Limnol. Oceanogr. 16 (1), 60-70. https://doi.org/10.4319/lo.1971.16.1.0060
- Pasulka, A.L., Landry, M.R., Taniguchi, D.A.A., Taylor, A.G., Church, M.J., 2013. Temporal dynamics of phytoplankton and heterotrophic protists at station ALOHA. Deep-Sea Res. Pt. II 93, 44-57. https://doi.org/10.1016/j.dsr2.2013.01.007.
- Patching, J.W., Eardly, D., 1997. Bacterial biomass and activity in the deep waters of the eastern Atlantic - evidence of a barophilic community. Deep-Sea Res. Pt. I 44 (9-10), 1655-1670. https://doi.org/10.1016/S0967-0637(97)00040-X.
- Pernice, M.C., Forn, I., Gomes, A., Lara, E., Alonso-Sáez, L., Arrieta, J.M., del Carmen Garcia, F., Hernando-Morales, V., MacKenzie, R., Mestre, M., Sintes, E., Teira, E. Valencia, J., Varela, M.M., Vaqué, D., Duarte, C.M., Gasol, J.M., Massana, R., 2015. Global abundance of planktonic heterotrophic protists in the deep ocean. ISME J. 9 (3), 782-792.
- Pernice, M.C., Giner, C.R., Logares, R., Perera-Bel, J., Acinas, S.G., Duarte, C.M., Gasol, J. M., Massana, R., 2016. Large variability of bathypelagic microbial eukaryotic communities across the world's oceans. ISME J 10, 945-958. https://doi.org 10.1038/ismej.2015.170.
- Perry, M.J., Eppley, R.W., 1981. Phosphate uptake by phytoplankton in the central North Pacific Ocean. Deep-Sea Res. Pt. A 28 (1), 39-49. https://doi.org/10.1016/0198 0149(81)90109-6.

- Redfield, A.C., Ketchum, B.H., Richards, F.A., 1963. The influence of organisms on the composition of seawater. In: Hill, M.N. (Ed.), The Sea: Ideas and Observations on Progress in the Study of the Seas, Volume 2. Interscience, New York, pp. 26–77.
- Reinthaler, T., van Aken, H., Veth, C., Arístegui, J., Robinson, C., Williams, P.J.I.B., Lebaron, P., Herndl, G.J., 2006. Prokaryotic respiration and production in the mesoand bathypelagic realm of the eastern and western North Atlantic basin. Limnol. Oceanogr. 51 (3), 1262–1273.
- Rii, Y.M., Karl, D.M., Church, M.J., 2016. Temporal and vertical variability in picophytoplankton primary productivity in the North Pacific Subtropical Gyre. Mar. Ecol. Prog. Ser. 562, 1–18. https://doi.org/10.3354/meps11954.
- Rii, Y.M., Peoples, L.M., Karl, D.M., Church, M.J., 2022. Seasonality and episodic variation in picoeukaryote diversity and structure reveal community resilience to disturbances in the North Pacific Subtropical Gyre. Limnol. Oceanogr. 67 (S1) https://doi.org/10.1002/lno.11916.
- Riley, G.A., 1970. Particulate organic matter in seawater. In: Russell, F.S. and Yonge, M. (Eds.), Advances in Marine Biology, Vol. 8. Academic Press, New York, NY, pp. 1–118
- Sakshaug, E., Holm-Hansen, O., 1977. Chemical composition of Skeletonema costatum (Grev.) Cleve and Pavlova (Monochrysis) Lutheri (Droop) Green as a function of nitrate-, phosphate-, and iron-limited growth. J. exp. Mar. Biol. Ecol. 29 (1), 1–34. https://doi.org/10.1016/0022-0981(77)90118-6.
- Segura-Noguera, M., Blasco, D., Fortuño, J.-M., Hwang, J.-S., 2016. Taxonomic and environmental variability in the elemental composition and stoichiometry of individual dinoflagellate and diatom cells from the NW Mediterranean Sea. PLoS ONE, 11 (4), e0154050.
- Sharp, J.H., 1974. Improved analysis for "particulate" organic carbon and nitrogen from seawater. Limnol. Oceanogr. 19 (6), 984–989. https://doi.org/10.4319/ lo.1974.19.6.0984.
- Sheldon, R.W., 1972. Size separation of marine seston by membrane and glass-fiber filters. Limnol. Oceanogr. 17 (3), 494–498. https://doi.org/10.4319/
- Shibata, A., Ohwada, K., Tsuchiya, M., Kogure, K., 2006. Particulate peptidoglycan in seawater determined by the silkworm larvae plasma (SLP) assay. J. Oceanogr. 62 (1), 91–97. https://doi.org/10.1007/s10872-006-0035-9.
- Sieburth, J.M.N., Smetacek, V., Lenz, J., 1978. Pelagic ecosystem structure: heterotrophic compartments of the plankton and their relationship to plankton size fractions Limnol. Oceanogr. 23 (6), 1256–1263. https://doi.org/10.4319/ lo.1978.23.6.1256.
- Siegel, D.A., Dickey, T., Washburn, L., Hamilton, M.K., Mitchell, B., 1989. Optical determination of particulate abundance and production variations in the oligotrophic ocean. Deep-Sea Res. Pt. I 36 (2), 211–222. https://doi.org/10.1016/ 0198-0149(89)90134-9.
- Sohrin, R., Imazawa, M., Fukuda, H., Suzuki, Y., 2010. Full-depth profiles of prokaryotes, heterotrophic nanoflagellates, and ciliates along a transect from the equatorial to the subarctic central Pacific Ocean. Deep-Sea Res. Pt. II 57 (16), 1537–1550. https://doi. org/10.1016/j.dsr2.2010.02.020.
- Sorokin, J.I., 1971. On the role of bacteria in the productivity of tropical oceanic waters. Int. Revue ges. Hydrobiol. 56 (1), 1–48. https://doi.org/10.1002/ iroh.19710560102.
- Sorokin, Y.I., Kopylov, A.I., Mamaeva, N.V., 1985. Abundance and dynamics of microplankton in the central tropical Indian Ocean. Mar. Ecol. Prog. Ser. 24 (1–2), 27–41. https://doi.org/10.3354/meps024027.
- Steinberg, D.K., Van Mooy, B.A.S., Buesseler, K.O., Boyd, P.W., Kobari, T., Karl, D.M., 2008. Bacterial vs. zooplankton control of sinking particle flux in the ocean's twilight zone. Limnol. Oceanogr. 53 (4), 1327–1338. https://doi.org/10.4319/lo.2008.53.4.1327.
- Strathmann, R.R., 1967. Estimating the organic carbon content of phytoplankton from cell volume or plasma volume. Limnol. Oceanogr. 12 (3), 411–418. https://doi.org/ 10.4319/lo.1967.12.3.0411.

- Sutcliffe Jr., W.H., Sheldon, R.W., Prakash, A., 1970. Certain aspects of production and standing stock of particulate matter in the surface waters of the northwest Atlantic Ocean. J. Fish. Res. Bd. Canada 27 (11), 1917–1926. https://doi.org/10.1139/f70-217
- Swan, B.K., Martinez-Garcia, M., Preston, C.M., Sczyrba, A., Woyke, T., Lamy, D., Reinthaler, T., Poulton, N.J., Masland, E.D.P., Gomez, M.L., Sieracki, M.E., DeLong, E.F., Herndl, G.J., Stepanauskas, R., 2011. Potential for chemolithoautotrophy among ubiquitous bacteria lineages in the dark ocean. Science 333 (6047), 1296–1300. https://doi.org/10.1126/science.1203690.
- Utermöhl, H., 1931. Neue Wege in der quantitativen Erfassung des Planktons. (Mit besonderer Berücksichtigung des Ultraplanktons. Verh. Int. Verein. Theor. Agnew. Limnol. 5 (2), 567–595. https://doi.org/10.1080/03680770.1931.11898492.
- Verity, P.G., Robertson, C.Y., Tronzo, C.R., Andrews, M.G., Nelson, J.R., Sieracki, M.E., 1992. Relationships between cell volume and the carbon and nitrogen content of marine photosynthetic nanoplankton. Limnol. Oceanogr. 37 (7), 1434–1446. https://doi.org/10.4319/lo.1992.37.7.1434.
- Viviani, D.A., Karl, D.M., Church, M.J., 2015. Variability in photosynthetic production of dissolved and particulate organic carbon in the North Pacific Subtropical Gyre. Front. Mar. Sci. 2, Article 73. https://doi.org/10.3389/fmars.2015.0073.
- Watson, S.W., Hobbie, J.E., 1979. Measurement of bacterial biomass as lipopolysaccharide. In: Costerton, J.W., Colwell, R.R. (Eds.), Native Aquatic Bacteria: Enumeration, Activity and Ecology. ASTM International, West Conshohocken, PA, pp. 82–88.
- Watson, S.W., Novitsky, T.J., Quinby, H.L., Valois, F.W., 1977. Determination of bacterial number and biomass in the marine environment. Appl. Environ. Microbiol. 33 (4), 940–946. https://doi.org/10.1128/AEM.33.4.940-946.1977.
- White, A.E., Barone, B., Letelier, R.M., Karl, D.M., 2017. Productivity diagnosed from the diel cycle of particulate carbon in the North Pacific Subtropical Gyre. Geophys. Res. Lett. 44 (8), 3752–3760. https://doi.org/10.1002/2016GL071607.
- Williams, P.J. le B., Ducklow, H.W., 2019. The microbial loop concept: A history, 1930–1974. J. Mar. Res. 77 (2), 23–81.
- Williams, P.M., Carlucci, A.F., Olson, R., 1980. A deep profile of some biologically important properties in the central North Pacific gyre. Ocean. Acta 3 (4), 471–476.
- Winn, C.D., Karl, D.M., 1984. Laboratory calibrations of the [³H]-adenine technique for measuring rates of RNA and DNA synthesis in marine microorganisms. Appl. Environ. Microbiol. 47 (4), 835–842. https://doi.org/10.1128/AEM.47.4.835-842.1984.
- Winn, C.D., Campbell, L., Christian, J.R., Letelier, R.M., Hebel, D.V., Dore, J.E., Fujieki, L., Karl, D.M., 1995. Seasonal variability in the phytoplankton community of the North Pacific Subtropical Gyre. Global Biogeochem. Cy. 9 (4), 605–620. https:// doi.org/10.1029/95GB02149.
- Worden, A.Z., Nolan, J.K., Palenik, B., 2004. Assessing the dynamics and ecology of marine picophytoplankton: the importance of the eukaryotic component. Limnol. Oceanogr. 49 (1), 168–179. https://doi.org/10.4319/lo.2004.49.1.0168.
- Yamaguchi, A., Watanabe, Y., Ishida, H., Harimoto, T., Furusawa, K., Suzuki, S., Ishizaka, J., Ikeda, T., Takahashi, M.M., 2002. Structure and size distribution of plankton communities down to the greater depths in the western North Pacific Ocean. Deep-Sea Res. Pt. II 49 (24), 5513–5529. https://doi.org/10.1016/S0967-0645(02)00205-9.
- Yamaguchi, A., Watanabe, Y., Ishida, H., Harimoto, T., Furusawa, K., Suzuki, S., Ishizaka, J., Ikeda, T., Takahashi, M.M., 2004. Latitudinal differences in the planktonic biomass and community structure down to the greater depths in the western North Pacific. J. Oceanogr. 60 (4), 773–787. https://doi.org/10.1007/s10872-004-5770-1.
- Zweifel, U.L., Hagström, Å., 1995. Total counts of marine bacteria include a fraction of non-nucleoid-containing bacteria (ghosts). Appl. Environ. Microbiol. 61 (6), 2180–2185. https://doi.org/10.1128/AEM.61.6.2180-2185.1995.